OSLO

OSLO METROPOLITAN UNIVERSITY
STORBYUNIVERSITETET

Master's Degree in
Structural Engineering and Building Technology
Department of Civil Engineering and Energy Technology

MASTER THESIS

THESIS TITLE	DATE
Finite element model updating of a stone masonry tower using 3D laser scanner and accelerometers	15.06.2020
	NUMBER OF PAGES
	86/101

AUTHOR(S)	SUPERVISOR(S)
AGON ADEMI	M. KIOUMARSI and A. SHABANI

IN COLLABORATION WITH	CONTACT PERSON

SUMMARY

Two-part study, with operational modal analysis performed on a historic masonry tower located in Tønsberg, Norway based on ambient vibration testing with the use of accelerometers. Furthermore, a calibration of the data extracted from the ambient vibration testing towards numerical models of the same tower. In addition to this, the use of terrestrial 3D laser scanner was implemented to scan the tower for the use in FE analysis. The finalized calibrated models were compared and distinguished with the use of soil-structure interaction and without it. Moreover, important theory and previous studies of the different fields are presented.

3 KEYWORDS
OMA
FEM
Stone Masonry

Foreword

This thesis is a final part of the two-year master's degree program in *Structural Engineering and Building Technology*, at the Oslo Metropolitan University in Oslo, Norway. The scope of the thesis is equivalent to 30 credits and was carried out in the spring semester of 2020.

The author wants first and foremost to thank the two supervisors: Amirhosein Shabani and Mahdi Kioumarsi for the help and insightful guidance throughout the work with the thesis. In addition, thanks to Haidar Hosamo for the help with the laser scanning and useful information. Thanks also the Slottsfjell museum in Tønsberg for allowing several visits for both the laser scanning and ambient vibration testing inside the tower.

The ongoing Covid-19 pandemic (2020-) had a negative effect on the work that was initially planned for this thesis. Delays on deliveries of equipment and closed campus cased a lot of the work to be postponed, resulting in much shorter working time with data. Nevertheless, the work and results presented is archived because of good help and guidance by the two supervisors.

Agon Ademi

date & place:
15/06/2020, Oslo

_____

Abstract

This study's main objective was to investigate the dynamic response of the ancient masonry stone tower Slottsfjelltårnet located in the oldest city of Norway, Tønsberg. The study takes in use several fields in the process for the extraction of the dynamic response of the tower and the calibration of it in a finite element software.

The emphasis on finding the dynamic response of heritage structures using nondestructive tests and without hindering the daily operations paved the way to use operational modal analysis, which allows for attaining the dynamic characteristics without interfering with the daily activities of the structure.

The study was carried out with the initial scanning and mapping on the inside and outside of the tower with the use of 3D laser scanners. This data was used to model the structure in the building information modeling software, Autodesk Revit. The model was in turn imported into the finite element software Diana FEA, which was used for analysis and later calibration.

Secondly, the core part of the study took in use ambient vibration testing and operational modal analysis to extract the dynamic characteristics of the tower in operational conditions. Accelerometers were placed on the structure which gave readings that were then processed, which sequentially gave the dynamic behavior of the tower.

The third and final part of the study included both the modeling of the structure and the results from the operational modal analysis and ambient vibration testing in order to calibrate the finite element model, according to the extracted data. The process was performed on two different models with the use of soil-structure interaction and without it, where the different methods were modeled and evaluated. Results were then compared, where the material properties and other aspects were presented for comparison.

The procedure of operational modal analysis, with ambient vibration testing and modeling of the structure using 3D laser scanners is assessed towards available literature. Furthermore, previous studies and theory concerning the main aspects of the study are also presented.

Sammendrag

Hovedformålet med denne studien var å undersøke den dynamiske responsen til det gamle mursteintårnet Slottsfjelltårnet som ligger i den eldste byen Norge, Tønsberg. Studien tar i bruk flere felt i prosessen for finne den dynamiske responsen til tårnet og kalibrering av den i et analyseprogram som benytter elementmetoden.

Vektleggingen av å finne den dynamiske responsen til historiske konstruksjoner gjennom bruk av ikke-destruktiv testing og uten å hindre den daglige driften, banet vei for å bruke operasjonell modal analyse, som gjør det mulig å finne den dynamiske responsen uten å forhindre de normale driftsforholdene til konstruksjonen.

Studien ble utført med den innledende skanning og kartlegging på innsiden og utsiden av tårnet med bruk av 3D laserskannere. Disse dataene ble brukt til å modellere tårnet i bygningsinformasjonsmodellering-programvaren, Autodesk Revit. Modellen ble videre importert til elementmetode-programmet, Diana FEA som ble videre brukt til analyse, og senere kalibrering.

Hoveddelen av studien tok i bruk operasjonell modal analyse for å finne ut den dynamiske responsen til tårnet under normale driftsforhold. Akselerometer ble plassert på tårnet som ga avlesninger, som deretter ble behandlet og videre ga den dynamiske responsen til tårnet.

Den tredje og siste delen av studien inkluderte både modelleringen av tårnet og operasjonell modal analyse for å kalibrere elementmetode-modellen, i henhold til de ekstraherte dataene. Prosessen ble utført på to forskjellige modeller ved bruk av jordstrukturinteraksjon og uten den, der de forskjellige metodene ble modellert og evaluert. Resultatene ble deretter sammenlignet, der materialegenskapene og andre aspekter ble presentert for sammenligning.

Prosedyren med operasjonell modal analyse, vibrasjonslesing og modellering av konstruksjonen gjennom bruk av 3D laser skannere, blir vurdert i forhold til tilgjengelig litteratur. Videre presenteres tidligere studier og teori om hovedaspektene ved studien.

Table of Contents

_____

Abbreviations

AVT	Ambient Vibration Test
BFD	Basic Frequency Domain
BIM	Building Information Modelling
DFT	Discrete Fourier Transform
DTFT	Discrete Time Fourier Transform
EMA	Experimental Modal Analysis
FE	Finite Element
FEM	Finite Element Method
FFT	Fast Fourier Transform
FRF	Frequency Response Function
FS	Fourier Series
FT	Fourier Transform
IFC	Industry Foundation Classes
MDOF	Multiple Degree of Freedom
OMA	Operational Modal Analysis
PP	Peak Picking
PSD	Power Spectral Density
SDOF	Single Degree of Freedom
SSI	Soil-Structure Interaction
SSI	Stochastic Subspace Identification
SSSI	Structure Soil-Structure Interaction
STEP	Standard for the Exchange of Product Data

Figures List

_____

_____

Appendix

A

B

C

D

Tables List

Problem Statement

The problem statement of this thesis is to use the of operational modal analysis (OMA) and ambient vibration testing (AVT) on the stone masonry tower "Slottsfjelltårnet" (English: Castle Hill Tower) located in the oldest city of Norway, Tønsberg [1]. In addition to modeling a finite element (FE) model of the same tower, calibrated through the data collected from the implementation of OMA and AVT.

The purpose of the thesis will be to achieve the dynamic characteristics based on OMA with the use of sensors (accelerometers) without hindering the daily operations of the tower. Furthermore, a FE model is made using the FE software Diana FEA [2] and 3D laser scanners. The resulting outcome is to provide an optimal FE model which will accurately represent the dynamic behavior of the tower and be further used in future analysis of it.

Chapter 1: Introduction

The cultural, religious, and collective history of human evolution is reflected through our heritage structures. These structures range from cathedrals and mosques to old bell towers and museums. While they are old, the importance of them for architectural and engineering history is essential to preserve for future generations. In addition, many of these structures have huge cultural and religious importance not only for history purposes but also for tourism, as they serve as a direct economic contribution for many countries.

The degradation of heritage structures through natural hazards is uncontrollable however, the emphasis to prolong the life of these structures through monitoring and planned interventions is of utmost importance for the preservation of them. The development of software and hardware to serve as a tool for the preservation of heritage structures through the means of monitoring has over the few years progressed [3]. The use of ambient vibration testing (AVT) and operational modal analysis (OMA) has made it easier both to find the dynamic response of vulnerable structures, but also the continuous monitoring of them to prevent failure in the design integrity.

1.1 Objectives

The main objective of this research is to evaluate and investigate the use of OMA and AVT on the historical masonry Slottsfjell tower and acquire the dynamic response of it. This information will be used to produce different FE models based on material from previous studies and information obtained from the tower itself.

FE software will be used to evaluate different numerical models and assess them towards the acquired AVT data. Furthermore, the use of 3D laser scanners for the purpose of modelling historical structures is evaluated, discussed, and implemented in the research.

The secondary objectives of the research are to conduct a literature review on the different aspects of the study, related to the masonry material, numerical modeling of masonry, in addition to signal processing and OMA, among others. Moreover, the material models available to assess masonry and material properties will be reviewed, evaluated, and compared with the use of FE software. Different aspects such as the soil and foundation will also be presented and compared.

1.2 Thesis Procedure

Figure 1 shows a flowchart of how this thesis is going to be approached with the use of the OMA, FE model and 3D laser scanners.
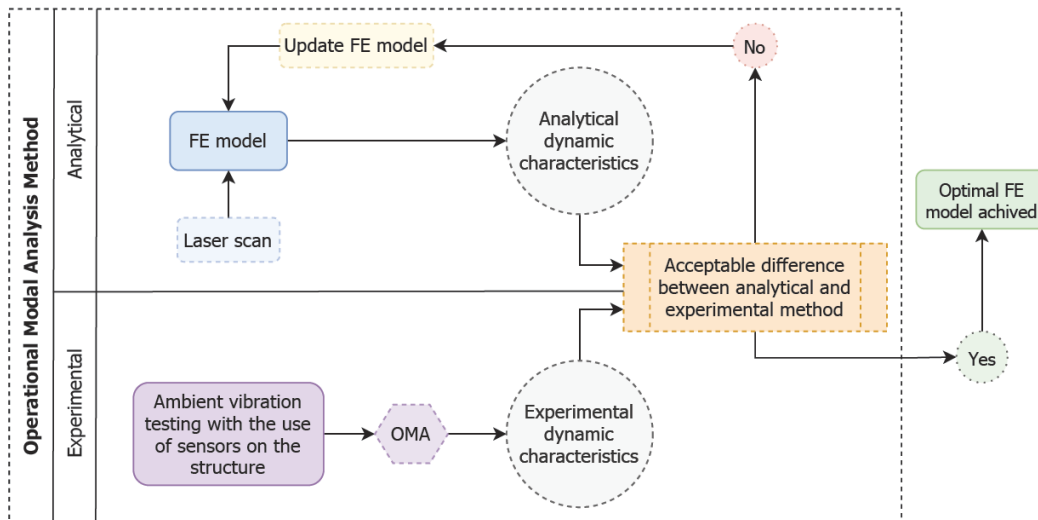
Figure 1 Flowchart - thesis procedure

The thesis is divided in four main stages, as shown in the flowchart above, and presented in the text under.

I. **FE model with the use of laser scanner**
A FE model is modelled, where the dynamic characteristics of the tower are extracted. To achieve accurate geometry of the tower, 3D laser scanners are used in the mapping of it.

II. **Ambient Vibration Testing**
The use of accelerometers and AVT is implemented to determine the dynamic characteristics of the tower, under normal daily operations of it.

III. **Comparing analytical and experimental results**
The analytical and experimental data achieved from the FE model and the AVT respectively, are compared and evaluated.

IV. **Updating FE model**
The difference between the analytical and experimental data is compared and evaluated. If the desired precision is not there, then the FE model is updated manually. The procedure is from point (**III**) executed as many times as necessary until the wanted precision is achieved and the model is optimal.

1.3 Thesis Structure

This thesis contains eight chapters and four appendixes. Short descriptions of each chapter are given as follows:

Chapter 1 Introduction:

The first chapter gives an introduction on the thesis procedure and overview of the work that is to be presented. In addition, the structure of the thesis is explained.

Chapter 2 Background:

The second chapter gives a theoretical basis of OMA and structural dynamics, in relation to dynamic response of systems. Signal processing for the purpose of extracting the modal parameters is also explained. Furthermore, the chapter also includes theory about masonry as a material, and numerical modeling of it, in addition to a general basis of the use of 3D laser scanners. Lastly the chapter also includes general background of previous studies in the different fields that are explained.

Chapter 3: Case study

The third chapter gives an overview of the case study that is the basis of this thesis, with background information about the tower itself.

Chapter 4: Geometrical Survey

The fourth chapter includes the geometrical survey of the tower, where an initial visual inspection is given. The chapter explains the process of 3D laser scanning and mapping of the tower for the purpose of modelling. Finally, it also gives the basis for the modelling of it and the process of converting the point cloud data to the final geometry.

Chapter 5: Numerical Modelling

The fifth chapter consists of the process of taking the geometrical model and converting it into a numerical model for FE analysis. The chapter includes an overview and specifics of the procedure used to alter the model and finally perform modal analysis on it. In addition to presenting the final discretized model, it also shows the results for the initial modal analysis performed on the numerical model, as well as gravitational analysis for verification of it.

_____

Chapter 6: AVT

The sixth chapter gives the basis of the AVT on the tower, where the procedure is presented as well as the results. The chapter includes the strategy used for the testing and theoretical background for the decisions made in relation to the placement and number of sensors, in addition to the time interval for the readings.

Chapter 7: FE Model Calibration

The seventh chapter considers all the previous chapters for the basis and procedure of calibrating and updating the FE models. The method used for the updating of the models, as well as theoretical background is presented. Finally, the results of the modal analysis for the calibrated models is presented for both linear and nonlinear material models.

Chapter 8: Conclusion and Future Work

The final chapter concludes with final remarks of the work presented, in addition to future works.

Appendixes

A
Appendix A gives an overview of the sensor specifications

B
Appendix B presents the results from the initial and second AVT readings

C
Appendix C gives an overview of the software used in the processing of the raw AVT data

D
Appendix D presents photos taken during the AVT readings and 3D laser scanning

Chapter 2: Background

2.1 Modal Analysis

The assessment of the dynamic response of civil structures is done with the use of modal analysis. There are several methods of performing structural dynamic testing on a given structure, to achieve the dynamic characteristics. These different methods can be divided into two main groups; 1) Forced-, and 2) AVT [4].

Modal analysis allows for attaining the modal shapes, natural frequencies and damping ratios of a given structure [5]. These elements can then be used to formulate a mathematical model for its dynamic behavior [6].

2.2 Operational Modal Analysis

The assessment of the dynamic response of historical structures has emphasized the need for this to be done in such a manner, which does not rely on physical tests on the structure itself. As historical structures are important to the local and national history and heritage of individual areas, the conservation of these structures is utmost important. Knowing the seismic vulnerability of these structure will help to maintain them for future generations. Necessary measures can be taken to reinforce vulnerable areas and help the preservation of them.

As explained in the previous section there are two main methods for the extraction of the dynamic response of structures. While the first method requires the modal parameter identification to be carried out based on both input and output measurement data, the second method will only base it on the out-put data, which is the case of the OMA. Figure 2 shows a general flowchart of the approach of the OMA.
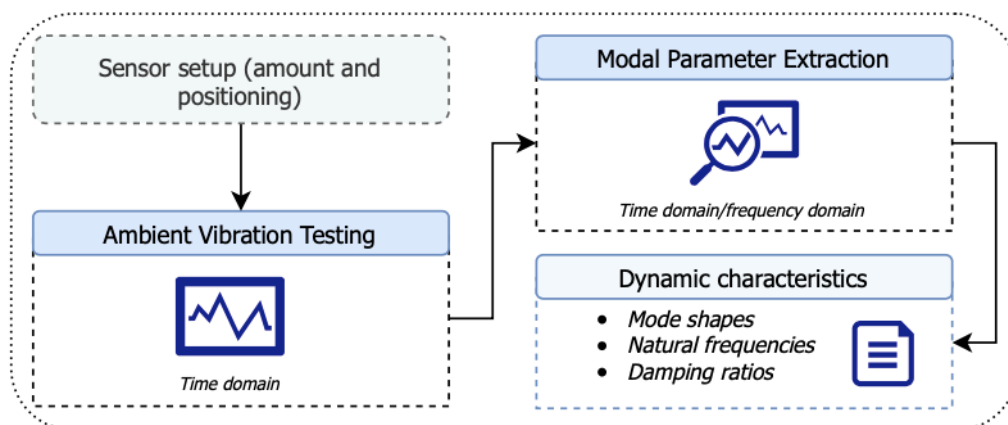
Figure 2 OMA approach

The development of hardware and software in the fields of AVT and OMA has over the last years strengthen the use of them, when dealing with heritage structures. While the use of them has made it easier regarding these structures, there are also a lot of key point of interest that distinguishes the different approaches to the methods. These differences in the approaches and methods used when implementing OMA and AVT range from the intention of the use (health monitoring, repair & retrofitting, seismic assessment) to the methods of extraction of modal parameters. Other important factors are sensor placement, damage identification of the structure and the execution of the AVT. All of the above mentioned factors are to be discussed in this thesis, however readers are advised to look at more comprehensive reviews such as [3].

In summary OMA can be explained as a method of analyzing the modal properties of a certain system under normal operational conditions [7]. Sensors are used to register output data of the structure based on the operational excitation. This excitation comes from the different actions which the structures are exposed to. The actions have different sources under normal operating conditions such as wind, human walking, waves or traffic. These actions contribute to subjecting the structure to what we call ambient vibrations, which are then measured with the use of sensors.

OMA has been implemented and used in a diverse set of studies of different structures to determine the dynamic characteristics. Most of the studies carried out in Norway, have applied OMA on bridges. This has shown to be of most interest in relation to resonance effects on them.

One study was carried out for the under-construction cantilever Dolmsundet Bridge, where two accelerometers where used [8]. The accelerometers were placed on the cantilever of the bridge deck, thus changing in the four stages of the bridge's construction. The result of the study was the extraction of the natural frequencies in the different construction phases with the use of Cov-SSI method. Another study was carried out for the proposed ferry free project on the E39 of the Norwegian west coast, where several methods of OMA where implemented through the use of MATLAB [9]. The methods were verified on two simple shear frames, where the dynamic characteristics were already known, based on previous studies. The methods were then implemented on the Hardanger Bridge, where actual measurement data was available. The results of the studies showed that the different methods gave good estimates, while the more advanced ones had somewhat higher precision, than the others. The study concluded that the Cov-SSI method was the best one, for the estimation of the dynamic characteristics.

Additionally, a study was done on the monitoring of the Bergsøysund Bridge, an end supported floating pontoon bridge [10]. The monitoring system consisted of a total of 14 accelerometers and was carried out successfully, where the system

identification was achieved. As also presented in [8, 9], the best method for the estimation of the natural frequencies, damping ratios and mode shapes was Cov-SSI.

Other implementations of OMA on structures in Norway have also been carried out. One case is a study for where the dynamic identification on a steel pantograph was done using OMA. The pantograph that was assessed was similar to ordinary pantographs used for the transfer of electric power from the catenary system to the train's motors. In this case, an FE model was modeled, which was compared and adjusted to the OMA experimental data, in order to achieve an accurate representation of the structure itself [11]. The study showed that the model that was calibrated with the data from the AVT, behaved in a similar manner to a physical model.

One of the main problems with the OMA when it comes to the data, is the maintenance of the data acquisition system. Furthermore other factors that need to be taken into account when using OMA are the planning, setting up and performing of the measurements in a fast and smooth fashion, as these in many cases cannot be redone [12] .

2.2.1 Transfer Path

The excitation on the structure is usually assumed to be approximately Gaussian white noise [13]. This white noise covers the frequency range of the modal characteristics of the structure, as it is distributed over a wide frequency range [7]. Figure 3 shows the conceptual transfer path of OMA, where the input includes a loading filter which can be explained as:

 The assumed white noise is not always white, and therefore we consider these "colored loads" as the output of an imaginary loading filter which is loaded by white noise.
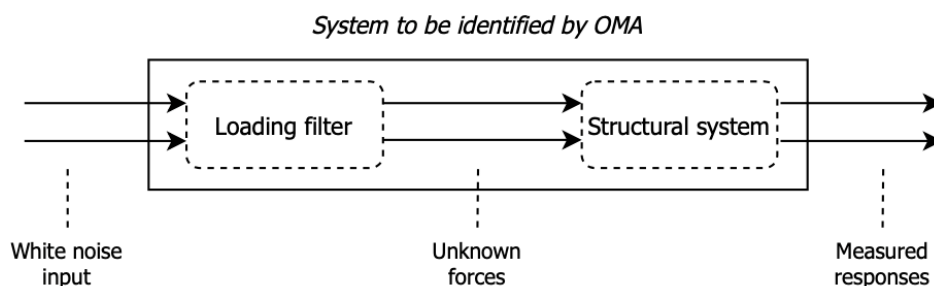
Figure 3 Conceptual transfer path of OMA

The loading filter does not alter the properties of the structural system, however the system that is to be identified needs to be estimated for the whole approach.

Therefore, when considering both the loading system and the structural system there will be structural and loading "modes".

Some of the assumptions that are made with the use of the OMA are [14]:

- The response of the system is equal to the input for a given combination of inputs.
- The structural dynamics of a system do not change over time, and therefore the system is not time dependent.
- The sensor layout is properly chosen to measure the response, and not place in node points.

2.2.2 Classic Modal Analysis

As explained above, the identification of the modal properties can be done through several different processes. While OMA does not rely on knowing the input, the actual excitation is therefore uncontrollable and unforeseeable. This is not the case for the classical experimental modal analysis (EMA). The EMA method uses physical properties of experimental measurements (controlled input that is measured) of the system/structure to correlate the dynamic characteristics of a mathematical model [7].

The use of sensors and no interference with the operation of a structure is a key factor for why OMA is specifically suitable for structures with historical value, as it allows for attaining dynamic characteristics without doing any destructive tests on the structure itself. Classical modal analysis such as EMA is however not suitable for historical structures, because of the required input measurement [15].

The main advantages of the OMA compared to the EMA are [16]:

a) Because the input is not measured, the procedure is cheaper and faster.
b) The procedure does not interfere with normal operation of the given structure.
c) The resulting response that is measured gives a good representation of the actual operating conditions of the given structure.

2.3 Structural Dynamics

The following chapter will give an introduction and overview of the fundamental concepts of structural dynamics for multi degree of freedom (MDOF) systems, and the damping of them. In addition, main aspects that are important for understanding the modal properties of different structures and systems, in relation to frequency and excitation is described.

2.3.1 Multiple degree of freedom system

Describing a MDOF system in matrix form can be done through the following formula:

$$[M] \{\ddot{y}(t)\} + [C] \{\dot{y}(t)\} + [K] \{y(t)\} = \{x(t)\} \qquad \textbf{(1)}$$

Where, [M], [C], and [K] are the mass, damping, and stiffness matrices. $\ddot{y}(t)$, $\dot{y}(t)$ and $\{x(t)\}$ are the vectors of acceleration, velocity, and displacement, respectively, while $\{x(t)\}$ is the force vector.

Free response of an undamped system

If we consider a system where there are no external forces acting on it, in addition to very small damping forces, that can be neglected, then we are looking at a free response of an undamped system. In that case, the following can be considered: x(t) = 0 and C = 0.

Based on the damping of the system, the response of it changes. This is an important attribute when considering modal analysis in both FEM and experimental data. The effect of the damping is illustrated in figure 4 under, where the free response of undamped system is shown in green.
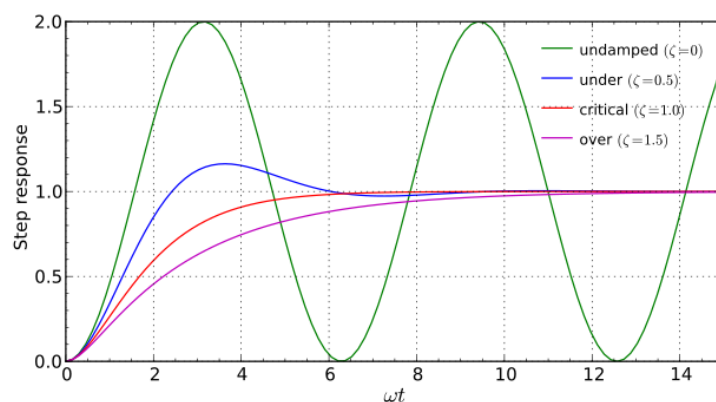
Figure 4 Damping influence on a system [17]

2.3.2 Natural Frequency

The natural frequency of a structure is the frequency for which the structure vibrates when it is disturbed (impacted by any action). For each structure or object there could be many natural frequencies. The number of degrees of freedom for a certain system is equal to the number of natural frequencies this system has.

2.3.3 Damping Radio

The damping ratio of a structure is a parameter explaining how a system's oscillations decay, after being disturbed. A system where there is no damping will therefore keep moving, without stopping.

2.3.4 Resonance

When the natural frequency of a structure is amplified, the structure will be exposed to resonance. This is done when the structure is impacted by an external action which is equal to the natural frequency. The resonance phenomena can be compared to a person on a swing that amplifies the swings height for each trust when exerting this force at the right time.

2.3.5 Period

The relation between frequency (Hz) and period (s) is given with the following formula:

$$f = \frac{1}{T} \qquad (2)$$

As presented in the formula above; the two properties frequency and period are inversely proportional to each other. In short, period is the time (in seconds) to complete one cycle of vibration and frequency (in hertz) is the number of completed cycles in one second, figure 5 illustrates this in a graph.
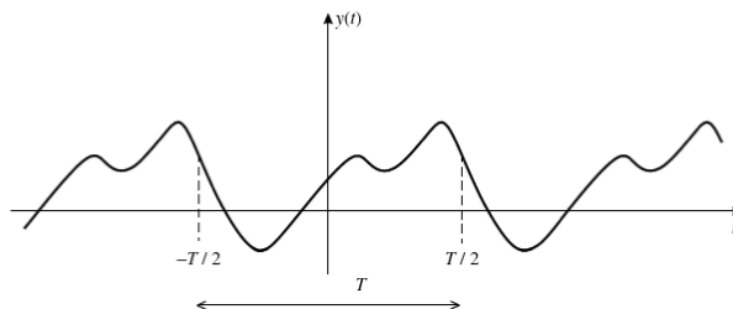
Figure 5 General periodic function [7]

2.3.6 Mode Shapes

The mode shapes for a given structure is the pattern of vibration for which the structure vibrates for a certain frequency. For different frequencies, these mode shapes change. Using modal analysis will make it possible to find these mode shapes and the corresponding frequencies.

Figure 6 presented a cantilever beam where the expected mode shapes are shown. As seen in the figure, the first two mode shapes are bending shapes, while the third is a double bending. Usually it is expected that the first mode shapes are simple ones, with the more complex ones such as torsional and double bending appearing in a higher frequency.

Of course, it is difficult to predict a natural frequency for a system without analyzing it with either modal analysis using sensors or with the use of modal analysis in a FE software. For systems that are much more complex than the one presented in the figure under, where there are a vast number of beams, columns and different material, the use of modal analysis is a necessary tool for extracting the mode shapes and the corresponding frequencies.

Mode shape and natural frequencies

Mode shape 1

Mode shape 2

Mode shape 3
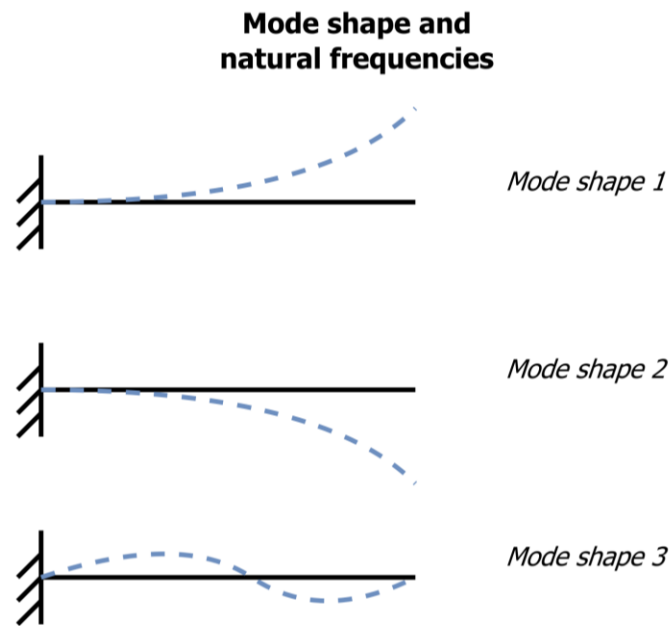
Figure 6 Modal shapes for a cantilever beam

2.4 Signal Processing and Modal Parameter Extraction

Understanding signals and the processing of them is important when dealing with modal analysis. This section is therefore going to give an overview of signal processing techniques through Fourier, in addition to modal parameter extraction.

One of the fundamentals to the signal processing in modal analysis is the Fourier transform, and it is one of the key milestones in the development in the technology of it. [6] Without the presents of the Fourier transform, the performing of modal analysis would not be possible.

2.4.1 Periodic Function

A periodic function can be defined by a function with the fundamental period T. In that case the following equation is true for any given periodic function:

$$f(t + T) = f(t) \qquad (3)$$

2.4.2 Fourier Series

Fourier series is a representation of a periodic function, given as the sum of infinite harmonically related sinusoids. With the formula given under, it is possible to compute any given periodic function.

$$g(t) = a_0 + \sum_{n=1}^{\infty} \left(a_n \cos \frac{2n\pi t}{T} + b_n \sin \frac{2n\pi t}{T} \right) \qquad (4)$$

2.4.3 Fourier Transform

As mentioned above, with the use of the Fourier Series it is possible to express a given signal in terms of the frequencies that make the sum of it. The Fourier Transform can be used to decompose functions, the formula is shown under and is given as a continuous function:

$$X(f) = \int_{-\infty}^{\infty} (t) e^{-2\pi i f t} dt \qquad (5)$$

2.4.4 Discrete Fourier Transform

The formula given for the Fourier transform is given from -∞ to ∞, however in practice this will not be the case, as there will be a given time interval that is

analyzed. While the Fourier Transform formula does not analyze a finite time interval, we use the Discrete Fourier Transform (DFT), which is shown under:

$$X(k) = \sum_{n=0}^{N-1} \left(e^{-\frac{2\pi ikn}{N}} \right) \qquad (6)$$

where $\frac{k}{N} = f, n = f$

As it is not possible to look at frequency and time continuously, the formula allows for calculating a summation of the frequency coefficient of a finite time interval. Figure 7, shows the DFT applied on a function, where the result is a set of discrete points that are summed according to the formula of the DFT.

Figure 7 Discrete Fourier transform [18]

The results of using the DFT and summing up all the parts is the following complex number, as given under:

$$X_k = A_k + B_{ki} \qquad (7)$$

This number can in the next step be plotted into a complex plane, while using the real and imaginary part of the number as coordinates. The numbers will together give information of both the magnitude and the angle of a vector, which in turn will give the necessary values to know the amplitude and phase shift of the sinusoid. Without going further into detail of the theorem, the idea of the Fourier transform is that a signal can be split into individual constituent frequencies.

A given periodic signal contains the sum of the elements at all frequencies [6]. Each of the frequencies will have a given power which together will give the total power of the signal.

2.4.5 Discrete-Time Fourier Transform

The Discrete-Time Fourier Transform is another form of Fourier analysis which is used for analyzing discrete data of a continuous function. The formula is given under.

$$X(f) = \sum_{n=\infty}^{+\infty} \left(e^{-\frac{2\pi i k n}{N}} \right) \qquad (8)$$

2.4.6 Fast Fourier Transform

In modal analysis the Fourier analysis can be used to compute the system's frequency response function, which in turn can be used to compute the modal parameters [19]. This is done using the Fast Fourier Transform (FFT).

The FFT has made huge changes in the computational techniques used in both filter simulation and spectral analysis, but also other related fields. The method is now widely used and is a technique for computing the DFT (see over) of a time series, rather effectively [20]. While the possibility for this to be done was also present before the application of FFT, it became more effective and cost efficient with the implementation of it.

While the method is not going to be explained in detail in this thesis, the use of it is based on calculating the coefficients of the DFT iteratively and thus saving a lot of computation time. Readers are advised to read Cooley and Tukey's initial publication of the algorithm for a more in depth explanation of the method [21].

2.4.7 Summary of Fourier

A summary of the different Fourier transforms is presented in table **1.** The distinction between the different transforms are that of the time duration, which can be divided into finite and infinite in addition to continuous or discrete functions.

Table 1 Fourier Summary

	Time interval	
	Finite	*Infinite*
Continuous	Fourier Series (FS)	Fourier Transform (FT)
Discrete	Discrete Fourier Transform (DFT)	Discrete-Time Fourier Transform (DTFT)

2.4.8 Modal Parameter Extraction

While the previous chapters have laid the foundation for the signal processing, the following paragraphs will explain the techniques that can be used to extract the modal parameters for AVT.

As there are many methods available, this thesis is only going to give an overview of the most common ones. Readers are advised to look for more specific literature for detailed insight in each of the methods.

Before going into detail on the different modal parameter extraction methods, there is one key aspect that needs to be explained. This is the concept of time domain and frequency domain. When talking about waves and frequencies it is normal to talk about wave amplitude given over time, also known as the time domain. However, it is also possible to talk about it in the frequency domain. In that case the wave amplitude is given over the frequency.

Both domains have their up and downsides. When looking specifically at the time-domain, one important characteristic is that the modes that are present in each signal, are also present at any time, figure 8 illustrates this. This is one of the drawbacks of the time domain, on the other side one of the benefits is that it is easier to obtain bias-free data, in comparison to the frequency domain.

Apart from this, when looking at the frequency domain and the use of it in modal parameter extraction, each mode has a small frequency band where it dominates, this can be seen in figure 8 as well. Thus, the frequency domain has an advantage in that the decomposition can be considered simply by looking at different frequency bands where the individual modes dominate. This gives the frequency domain the characteristic of natural modal decomposition, therefore making it much easier to distinguish each mode.
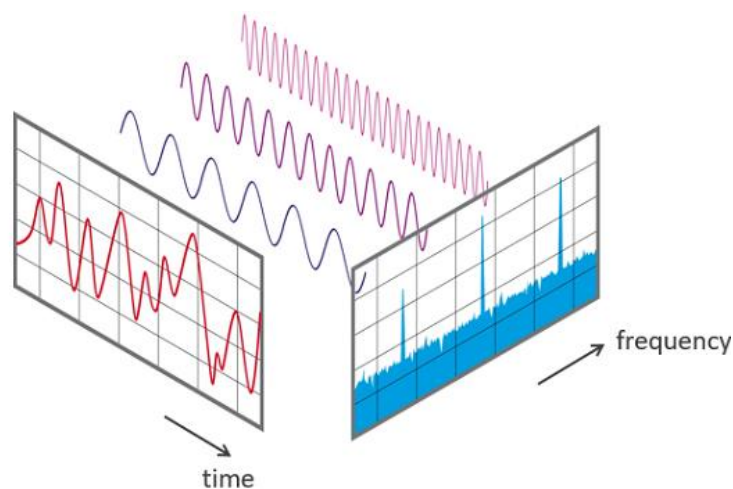

Figure 8 Frequency domain and time domain visualization [22]

Frequency Domain Method
Peak Picking (PP) Method

The peak picking (PP) or Basic Frequency Domain (BFD) method is one of the easiest methods used in modal analysis for output only measurements. The method is based upon that the frequency response function (FRF) reaches a "peak" or an extreme around the natural frequency, as also illustrated in figure 8.

The way the method is implemented is using the DFT where the measured time histories are converted to spectra. The natural frequencies are then determined as the spikes in the power spectral density (PSD) plot [23]. While the method allows for a fast implementation, it also has disadvantages in that the method is exposed to a subjective selection of natural frequencies. Furthermore, it lacks accuracy in the estimates of the deflected shapes of structures. The method's precision is also dependent on the frequency resolution of the spectral density and therefore the method only gives an estimate. Moreover the method is also influenced by noise [7].

The method can be classified as a SDOF method for OMA. With the use of the method, an assumption is made upon the resonance, that only one mode is dominant [14].

Time Domain Method
Stochastic Subspace Identification (SSI) Method

The Stochastic Subspace Identification method (SSI) is an output only method suitable for modal parameter identification in OMA. The method is compared to the PP method more complex.

The SSI method is used in the time domain, where there are a vast number of algorithms available. This allows the method to be implemented directly, without the use of spectra such as the PP method. The algorithms used will always produce a (sub-optimal) outcome, as a result of the algorithms being non-iterative and never ending in a local minima [24].

We divide the SSI method into two main types: the correlation driven SSI, and the data driven SSI. The correlation driven SSI also denoted Cov-SSI considers the problem of identifying the stochastic state space model, from the output data of the AVT. The data driven SSI, also called DD-SSI does on the other hand rely on linear algebra tools and mathematical framework in order to identify the state space matrices from the acquired raw data.

As this thesis is only going to give an overview of the method, readers are advised to read more detailed papers accessible to get a detailed explanation, such as [23] and [24].

2.5 Masonry

When looking at OMA implementation on historical masonry tower, there are a lot of studies available. Several studies have been implemented in Italy [5, 25]. These studies were carried out on historical bell towers, where there were used accelerometers to achieve the dynamic characteristics, successfully. Furthermore, both studies also developed FE models Abaqus software to predict the dynamic behavior. Modal analysis was performed on the FE models and tuned according to the results extracted from the ambient vibration measurements from the sensors, which resulted in a FE model that acted as predicted from the AVT data.

Studies have also been carried out for continuous monitoring of structures. A study in Italy assessed a stone tower in Perugia, for damage identification [26]. Other studies in Italy focus on the same thing, such as a two-part study carried out for historical masonry structures with continuous monitoring for the two towers; Gabbia and San Pierto, located in Mantua and Perugia respectably [27]. The study showed that with little number of accelerometers, it was possible to achieve the dynamic characteristics and perform damage detection on the structure.

Other studies have also been carried out in Portugal [28], this study specifically looked at two case studies. One of which was a clock tower built in the 16. century situated in the northeastern parts of Portugal. The other study was also carried out on a 16. century structure, which was a church located in the capital of Lisbon. Both structures were historical masonry constructions, where the dynamic characteristics were achieved with the use of sensors.

Similar studies have also been implemented on historical minaret in Turkey [29]. Where the results of AVT on the structure was used to update and optimize a FE model. The final FE model compared to the initial one, resulted in deviation from the experimental data to be reduced on average from 27 to 5 %.

In the available papers and literature, there are certainly many papers where OMA has been implemented. The method has been implemented for different structure types, and there are many papers concerning historical structures, and more specifically historical masonry.

2.5.1 Overview

Masonry is a composite material made up of units of different types, which are separated with a cement paste (or no paste in certain cases), see figure 9.
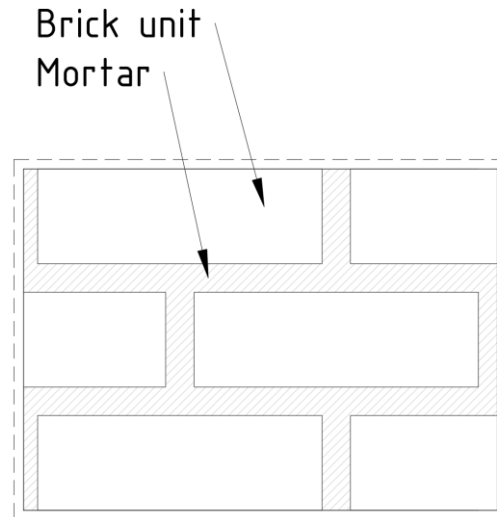
Brick unit
Mortar

Figure 9 Masonry material

Historically masonry has been used in a wide range of structures, ranging from bridges to towers, churches, and mosques. It is therefore often present in historical structures such as the one assessed in this thesis.

Masonry is a heterogeneous material with anisotropic properties, because of its structure. The joints in masonry structures are usually the weak points of them and most cracks appear in these areas [30]. In addition because of the irregular stone sizes in many stone masonry structures, the mechanical properties will show variation [31].

2.5.2 Damage on Masonry Structures

The main damage on masonry structures are usually connected to cracks, material degradation and deformations as well as foundation settlements [28]. Other damages present in masonry structures are related to spalling of the material, where brick simply is missing. Furthermore, the cracks can be of different character, depending on the actions the structure is subjected to.

Corner damage occurs because of poor wall-to-wall connections, while shear cracking usually happens in opening because of insufficient lateral strength [32]. Overall, in order to identify and document the full material health in masonry but also structures of other materials, both visual and testing (destructive or non-destructive) needs to be implemented.

2.6 Numerical Modeling

As explained in the previous section there are many studies carried out for the combined research of OMA and FE model calibration. Many of these studies are interesting regarding the importance of numerical modeling for the assessment of dynamic response of structure. While performing OMA will help achieve the dynamic characteristics, the numerical modeling will allow for implementing this knowledge of the structures and performing different analyzes on them based on that. The upcoming sections gives the basis of FEM and numerical modelling of masonry.

2.6.1 FEM

The FEM has developed into an essential technology in modeling and simulation present in a large amount of field. The method was initially implemented to solve problems related to structural analysis, but has since been used for thermal analysis and fluid flow analysis among other things.[33]

The FEM is a numerical method where the approximated solution is obtained by dividing the problem domain into small number of elements, and from there applying physical principle laws of these elements. When assessing specific structural analysis cases, the solving of problems can be very complicated when solving the main differential equations (dependent on geometry, material, boundary, loading conditions etc.) through the use of analytical means, therefore an approximation via FEM is an easier and less time-consuming option.

Computational modeling through the use of FEM can be divided into these steps [33]:

I. Geometrical modeling of the structure
II. Meshing (discretization) of the geometry
III. Specifying material properties
IV. Specifying boundary and initial conditions, as well as loading conditions

2.6.2 Modeling of Masonry

As the masonry material is not homogeneous, there are two key points that need to be considered when modeling masonry structures, regarding the structural behavior. These are: a) the behavior of the masonry units and b) behavior of the joint material [34].

We split the modeling of masonry structures into two main categories according to these two key points mentioned above, which are; micro modeling and macro modeling [34]. These two different categories are distinctive in that the micro modeling considers the presence of vertical and horizontal mortar joints, and in

_____

addition to that the material is anisotropic. While the macro modeling does not take this into account [35].

In general, when modelling historical structures such as the one assessed in this thesis, there are some issues that are present that needs to be evaluated [25]:

- Excessive simplifications of the modelling should be avoided.
- The FE models that are used without the validation of experimental data.
- There are a lot of uncertainties connected to the structural models even when all available data is collected.
- The connection between the results of local test and the quantitative parameters that are used to build a structural model are an open issue with no complete correlation.

While there are uncertainties connected to the modeling of historical structures, there are also a lot of different ways of modeling them. Depending on the intention of the modeling and the level of detail, these methods change. The next paragraphs will present the different ways of modeling masonry.

The two methods mentioned above can also include another intermediate approach, making it a total of 3 different approaches of refinement that can be taken when modeling masonry, as shown in figure 10 [34, 36]: These three methods take into account the complexity of the masonry structures in different scales. Depending on the scale of the structure that is to be modeled and the intention with the modeling, each of these methods has their benefits.
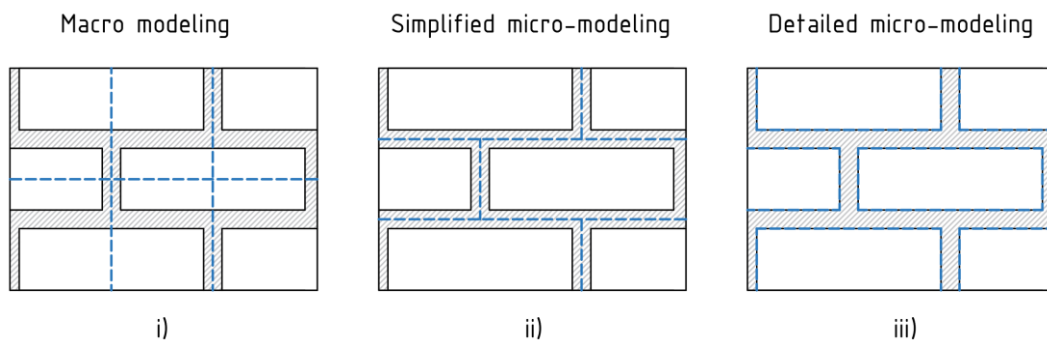
Figure 10 One, two- and three-phase modeling

i. One-phase material "*Macro modeling*"
   As seen in figure 10 i) in this method of refinement the material is modeled in continuum. There is no direct distinction between the different parts and therefore the material will act as a homogenous unit. Because there is no distinction of the different units, the method is not good for detailed stress analysis. However, it can be suitable for modeling of bigger masonry structures.

_____

ii. Two-phase material "*Simplified micro-modeling*"
The two-phase material method of refinement takes a bigger step into the micro modeling of the structure of masonry as seen in figure 10 ii). In this method, the different units are split in a way that considers the size of the brick units and the paste size. The method allows for a simplification of the complexity of the masonry material, while being more complex than the previous mentioned one-phase material method. When it comes to the interface between the different units, it is equal to the one phase material method in that the thickness of the joints is taken as zero. The method is applicable in a wide range of structures because of the allowed reduction in simplicity compared to the three-phase material method.

iii. Three-phase material "*Detailed micro-modeling*"
In this method the masonry material is modeled with continuous joints, while the bricks are modeled discontinuously as shown in figure 10 iii). The method allows for far more accurate results of the FEM model, but the complexity of the method also reduces the use of it because of computational effort needed to implement it. Micro-modeling requires that it includes all the failure mechanisms of material, cracking of joints, sliding over one head or bed joint, cracking of the units and crushing. [36]

The three presented methods of refinement can be seen as the three main different methods of modeling of masonry. The flowchart shown in figure 11 displays the diverse methods that can be taken when performing numerical modeling of masonry structures. This thesis will not go in depth on the methods in that level of detail, however a lot of literature is available that compare and investigate the different approaches available. [30, 34]
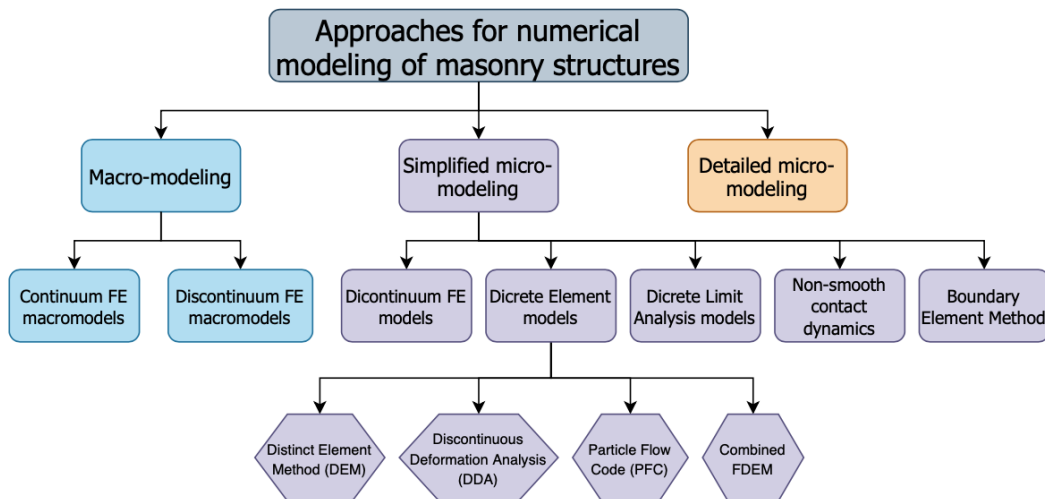

Figure 11 Approaches for numerical modeling of masonry structures

On the above-mentioned basis, a more simplified approach can be taken when looking at different modeling possibilities for numerical modeling of masonry

_____

structures. The intention of the modeling is the most important part of the approach that is selected, and the modeling approach needs to suit the purpose of it in order to get the wanted result.

Soil-Structure Interaction

An important aspect when modelling different structures directly on the soil is the interaction the soil has to the structure, and the behavior is causes. The soil-structure interaction (SSI) has been an essential part in earthquake engineering and has gained a lot of attention internationally in the last decades. The reason being the importance of It, when investigating the dynamic response of structures.

Using SSI has shown that when considering two identical structures, the response of that given structure differs a lot. For example considering a structure supported by a flexible soil, appose to a rigid base will give different response on the structure [37].

The application of SSI on numerical models, and how it differs from no SSI consideration is shown in figure 12. The two different approaches taken to define the supports of the structure differs in that the implementation of SSI takes into consideration the soil and the interaction of it with the structure itself. Whereas the numerical models without the application of SSI will not consider the interaction of the soil with the structure.
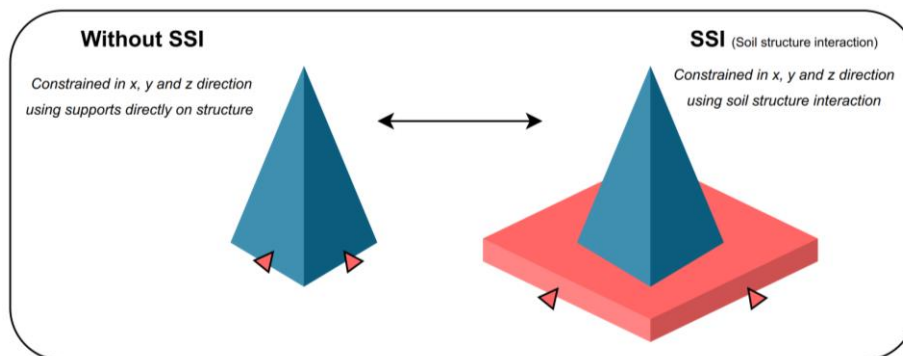

Figure 12 Numerical models with and without SSI implementation

As seen in the figure, the structure where SSI is not considered will neither consider the mechanical properties of the soil, but also not consider the interface between it and the structure. Therefore, the numerical model will be much simpler, but the response of it will also be altered as explained above.

Furthermore, the application of SSI has become much easier with the use of modern FE modelling software's such as Diana, where the interface interaction between the soil and the structure is defined effortlessly. This implementation will be explained in chapter 5 of the thesis.
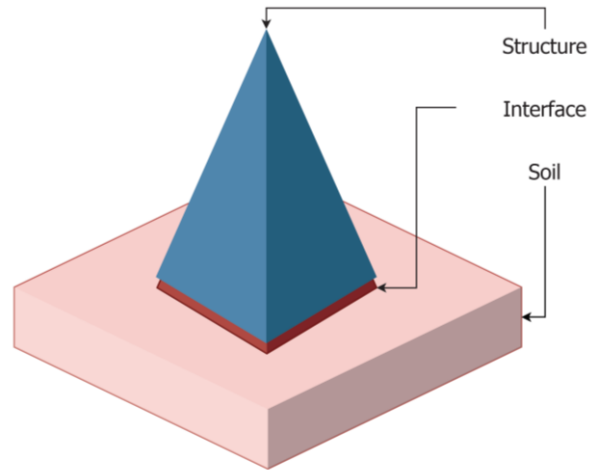
Figure 13 Visualization of SSI implementation

As explained above the interface of the structure and soil is the basis for the SSI method. Figure 13 shows the implementation of it on a given structure, where the FE model of the structure and the soil is defined with an interface in between them. The implementation of the method changes according to how the composition is, where the relation of the structure relative to the soil and vice versa can be different depending on each structure. The figure above is therefore only a simple sketch of the SSI implementation.

While the SSI method simply focuses on the interaction between the soil and the structure, in recent years the Structure-soil-structure interaction (SSSI) has gotten a lot of research attention [37]. The effects the structures have on each other based on the soil, can be assessed with the method using interfaces. This more complex interaction method is compared to SSI more important in a city scale point of view, where there is a dense structure presence.

The use of SSI in numerical modelling was for some time considered only beneficial in relation to the assessment of seismic vulnerability of structures. However, it has shown to lead to a larger than expected factor of safety and thus actually making it unsafe to use without the full knowledge of it [38]. The use of it, and the implementation for assessment of dynamic response is therefore important to examine and recognize thoroughly before implementing it.

Moreover, the difficulty of the implementation of SSI and the required input of it can make it difficult to fully execute. For this purpose, different methods and models have when proposed for structures with basement levels. [39] One of the applicable models with the implementation of basement levels, where the SSI effects had been neglected showed results close to the model with the consideration of SSI effects. [40] Thus, the application of simpler approaches is possible when considering the dynamic response.

2.7 3D Laser Scanning

When it comes to introduction of laser scanners in geometrical modeling of FE models, there are several studies that are interesting. The implementation of laser scanners used to present a semi-automatic procedure was the basis of a study performed in Italy [41]. The procedure presented converted the point clouds to three-dimensional geometry, that in turn could be imported into FE software. The study showed that the method and the corresponding procedure resulted in an effective and less time-consuming way for modeling the geometry of complex buildings, such as historical structures.

Laser scanners provide as an effective tool in visualizing different structures, which is especially important for more complex structures. The direct integration of laser scanners into FE software is however difficult to achieve, this particular issue is addressed in [42]. The paper describes the use of BIM (Building Information Modeling) models derived from point clouds for use in simulations in FE analysis. While most commercial BIM software's, such as Revit [43] and ArchiCAD [44] are usually used for managing and modeling of new buildings, they can also be utilized for other use cases. The paper presents how these kinds of software's can be used, even though they are somewhat lacking in the aspect of use in existing complex structures. The case-study presented in the paper is evaluated with different available literature for the conversion of points to geometrical model for use in FE analysis.

The implementation of laser scanner in the use of FE models have been used in other studies, such as the case of the historic bridge modelling, where the context of the study was structural dynamics [45]. The study that was carried out had in addition to laser scanning, also penetration radar for presentation of the geometry in use for the FE modeling. The resulting FE model was used in performing modal analysis. After analyzing the results achieved in this analysis it was seen that the extracted data from the analysis were good, when compared to other studies on similar structures.

While the direct conversion of point cloud into 3D geometry with high accuracy is shown to be difficult to achieve, there are studies carried out in this field. One study carried out in this arena, with the intention of using point-based voxelization for the conversion showed a good interpretation for the use in computational modeling [46]. The study was implemented with high degree of automation, however only for two-dimensional representation of solids. The study concluded with three key points for further evaluation to be used more widely: a) better shape detection of openings b) better distinction of real openings and c) higher level of automation, and emphasis on the expansion for full three-dimensional modeling.

The automatic implementation for point cloud conversion to a geometric model, which can be used in FE analysis is particularly important in more complex geometry. In these types of structures, a lot of time can be saved if the process is automatic, as well as it can eliminate human error. In [47] a methodology for the estimation of arches and vaults is presented, based on the symmetry of sections obtained along the vaults guideline. The acquired point clouds from the 3D laser scanners is accurately processed by statistical nonparametric methods, based on local bivariate kernel smoothers. The methods presented allows for an estimation of the cross sections of the arches, without the need of establishing parametric shape.

The implementation of 3D laser scanning for the purpose of FE analysis is also present in different types of available studies. While there are a vast amount of studies concerning these aspects, there are limitations in FE model calibration from OMA with the use of laser scanners on historical masonry towers, such as the one assessed in this thesis. This thesis is in that sense giving a quite broad and detailed specter of study, including all these aspects mentioned.

2.7.1 Overview

3D laser scanners allow for scanning and mapping 3D geometry such as buildings or objects for the purpose of importing this data into modelling software's. The use case of them is wide, as they can be used from illustrating the interior of a room, to more advanced deformation measurement of civil structures. Furthermore, there are a vast number of different 3D laser scanners available, from simpler terrestrial scanners to more advanced drones.

While the basis of the scanners is the same, the purpose of the use is different. For example, as mention in the previous section the data from the scanners can be used for automatic or semiautomatic conversion to 3D geometry, however this is still not fully developed. A more traditional way of using the scanners, is to take the point clouds from the measurement and use this as a template for the modelling.

Figure 14 shows a general overview of how terrestrial laser scanning is used to scan the 3D geometry of a structure. For the scans to be stitched together, each scan point needs to have shared points in between each order. These shared points are recognized by the software that is used to merge the scans into one model. The method and how the implementation of terrestrial 3D laser scanning is explained in depth in chapter 4, where an overview of the point clouds and the procedure is illustrated.
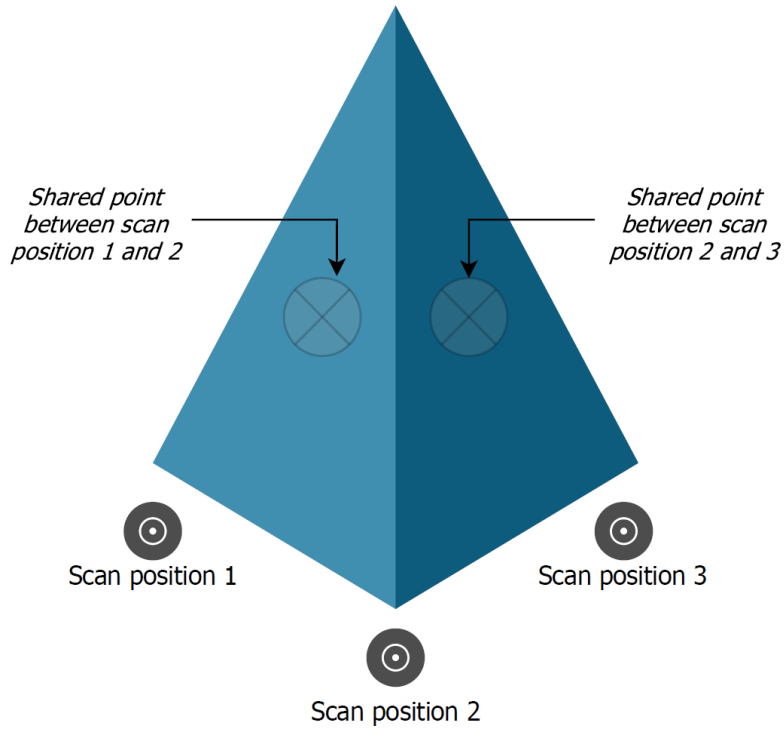
Figure 14 Terrestrial 3D laser scanning

Some key aspects that are important when working with terrestrial laser scanners are:

- The laser scanner needs to be calibrated for each scan point.
- More scans will give a denser grid of shared points and thus making it easier to merge the scans with a higher precision.
- The scanner will give a 360-degree scan but will have blank point at the base of the scanner, which needs to be considered.

It is important to choose the locations of the scans in relative to the size of the object that is to be scanned. A denser grid of scans is expected for interior of a house, opposed to scanning of a large tower.

Chapter 3: Case study

3.1 Overview

The Slottsfjell tower is located on a hill near the center of the city of Tønsberg in the southeastern parts of Norway, around 100 km south of the capital Oslo, see figure 15.

According to the Slottsfjell Museum, who have had the responsibility for the daily operation and dissemination of the Slottsfjell tower from the 1. of January 2012, they state the following on their official website:

> *The tower itself dates from 1888 but symbolizes the Slottsfjell area's connection to the Middle Ages. The tower is centrally located in the ruin park from what was once one of the largest medieval castles in the Nordic region* [22].
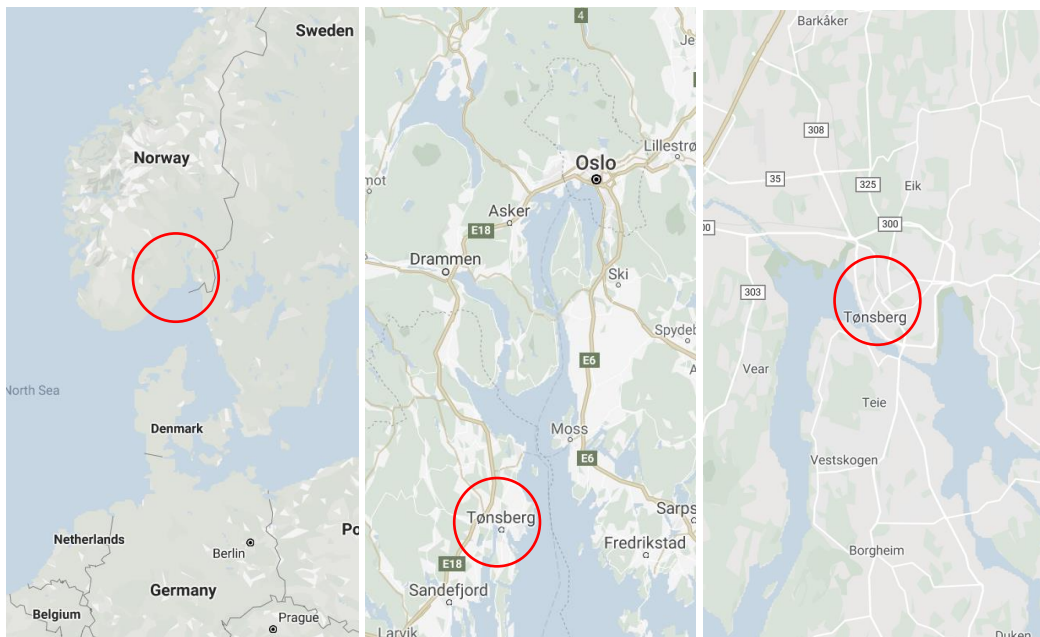

Figure 15 Slottsfjell tower situated in Norway

The tower is to the people living in the surrounding areas the key identification of the city of Tønsberg, and the county. The Slottsfjell tower is because of its high position, visible from large parts of the city. Figure 16 shows the Slottsfjell tower on top of the Slottsfjell hill, from the north-west side and south side.

Figure 16 Slottsfjell tower

The structure of the Slottsfjell tower is a typical medieval stone construction and does not distinguish itself much from the typical square shape of these kind of towers, as seen in figure 16 [48]. The tower has a total of four levels, where the final level is at the roof of the tower.

The Slottsfjell tower has a huge historical value to both the city of Tønsberg, but also the to the county of Vestfold and Telemark, because of the region's identification with the Viking Age. One example of this is the Oseberg skip, which was a ship from the Viking Age. The discovery is the most magnificent burial site from the Viking era in Norway [49].

Furthermore, the tower itself is not older than 150 years, as it was built to celebrate 1000 years since the city of Tønsberg was founded in 871. The text *871 – 1871* is also scripted on to the northside of the tower above the main entrance, with the corresponding text *"May the city that on the hill stand, flourish a thousand new years."*

_____

Chapter 4: Geometrical Survey

4.1 Visual Survey

In the first phase it is important to assess the tower and verify the structural integrity of it. This should be done with the use of available historic information, geometrical and topographic survey, in addition to damage surveys on the structure [28].

Generally, the process of using OMA for the structural identification of a given structure starts with the identification of the current overall health of the structure. This can be summarized in these overall steps [25]:

- Research and surveys connected to the historic evolution of the structure as well as collection all the essential data of the structure's geometry, in addition to the construction technology.
- Performing non-destructive (ND) test on the given structure to determine the characteristics of the materials.
- Visual inspection for the evaluation of the structure's preservation. The inspections aim is to map the crack patterns and irregularities, as well as difference in material and discontinuities.
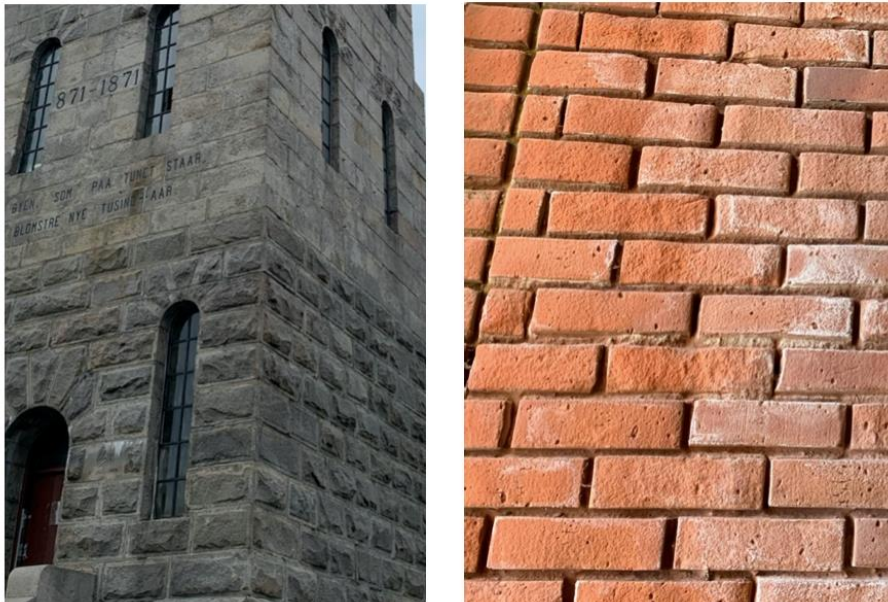

Figure 17 Material pattern and layout, outside and inside

Based on the age of the structure, the construction health has been determined by visual inspection only. From this visual construction survey, the following conclusions have been taken:

_____

- Overall construction health is good
- Masonry on the outside and inside shows good connections between mortar and unit block (see figure 17)
- There are no cracks or irregularities present that are visually identifiable (see figure 17)

On the above-mentioned conclusions, we assume that the FE model will be able to identify the dynamic behavior of the structure in a good way. Cracks and other complicated irregularities would contribute to making the model more complex and increase uncertainties. As these are not present in the FE model, the wanted results are easier achievable.

4.2 3D Laser Scan and Point Clouds

In order to model the tower in a proper way with all the necessary geometry, it was scanned with the use of terrestrial 3D laser scanner. The scanner used serve as an optical instrument and allows for a representation of an objects geometry, where the scans captures the three-dimensional space of the objects external surfaces [50].

The scanning allows for the corresponding point clouds to be imported and used in the FE modelling of the tower. The approach for the laser scans to the FE software is shown in figure 18.
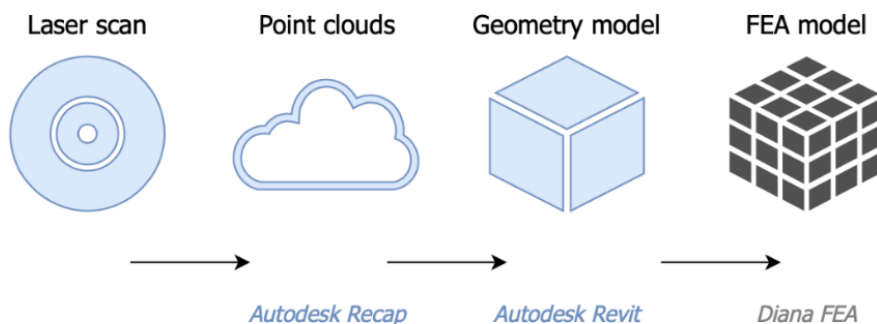

Figure 18 Laser scan and point cloud approach

The laser scanning was carried out with the GLS-2000 series 3D laser scanners [51]. Scanning was performed both on the outside and inside of the Slottsfjell tower with a total of 20 scans. For each individual scan, the laser scanner had to be calibrated and leveled, as shown in figure 19.

After finishing the laser scanning the scans where imported into Autodesk Recap [52] in order to combine them into one complete model. The software also allows for viewing individual scans and measuring them. For the combination of scans, 3 key points are needed to be identified for the software to combine them. The merging happens automatically after these points are detected. The marking of

the key points was performed for each of the scans, with several trials and errors before achieving the final combined 3D model.

Figure 19 3D laser scanner calibration

The resulting combined 3D model in Autodesk Recap is shown in figure 20, together with the scanning point. The scanning locations are marked on the figure as spheres. Scans performed on the inside of the tower are not visible in the figure due to the walls.

Figure 20 Recap 3D model of Slottsfjell tower

4.3 Geometrical Modelling

The laser scans and photos taken during the scanning where used actively in modelling the geometry of the tower. The modelling was performed in Autodesk Revit using the massing, more specifically the "model form" and "model void" options which models 3D solid and cuts 3D solids, respectively. The Recap model with the point clouds was imported into Revit and used to model the geometry of the tower. As the two software's are from the same developer, they are well integrated.

Figure 21 shows how the imported point clouds were used to model the geometry around the "real" structure, where the grey indicates the point clouds and the blue shows the modeled geometry.

Figure 21 Recap point clouds in Revit

While the Recap point clouds where good to identify the geometry it also had faults. The merged scans where not perfectly accurate, this is visible in figure 21 on the top part of the tower, where geometry is duplicated and located in different positions. These inaccuracies are present because the Recap software

did not achieve a perfect merging of scans, even though several trials were performed. To prevent this issue, more scans should have been made.

Regarding the above-mentioned challenges, some assumptions were made on the tower's geometry, which was used in the modeling:

- All angels in structural geometry were taken as 90 degrees
- Symmetry in opening and walls was assumed (windows and door openings were symmetric)
- Complex geometry such as the architectural column on the top of the structure were simplified

At this stage of the modeling, the only important factor was to model the geometry accurately, as this geometry will in the next step be important into the FE software Diana FEA. It is also important to note that the solids at this point do not have a mesh and have no properties, all these parameters will be defined directly in the FEA software.
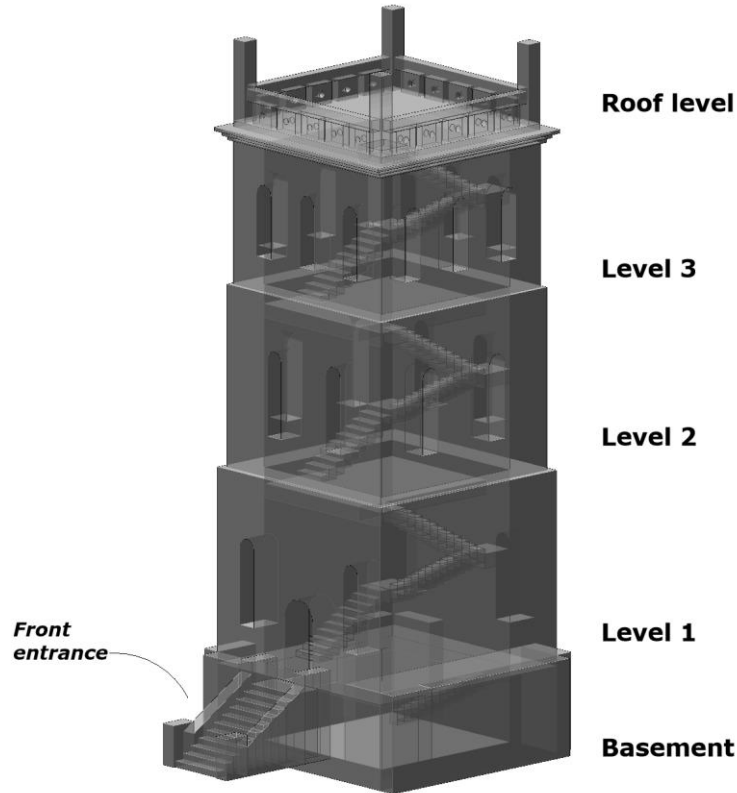
4.3.1 Final Geometry

Figure 22 Final Revit 3D model

The final geometry of the structure modeled in Revit is shown in figure 22, 23 and 24 with 3D and elevation views. The base of the tower is quadratic, and this follows the tower upwards, as shown in table 2, where the key dimensions are presented. Moreover, the dimensions are also available in one of the elevation views for more clear visualization.

Table 2 Key dimensions tower

Height	Dimension (m)
Total	21
Roof	2.4
Level 3	4.8
Level 2	5.4
Level 1	5.8
Basement	2.6
Width	Dimension (m)
Level 3	6.3x6.3
Level 2	6.5x6.5
Level 1	6.9x6.9
Basement	8x8

The final 3D model made in Revit is exported into the standard file format; IFC (Industry Foundation Classes). The importing of the model in the Diana software is explained in more detail in the next section.
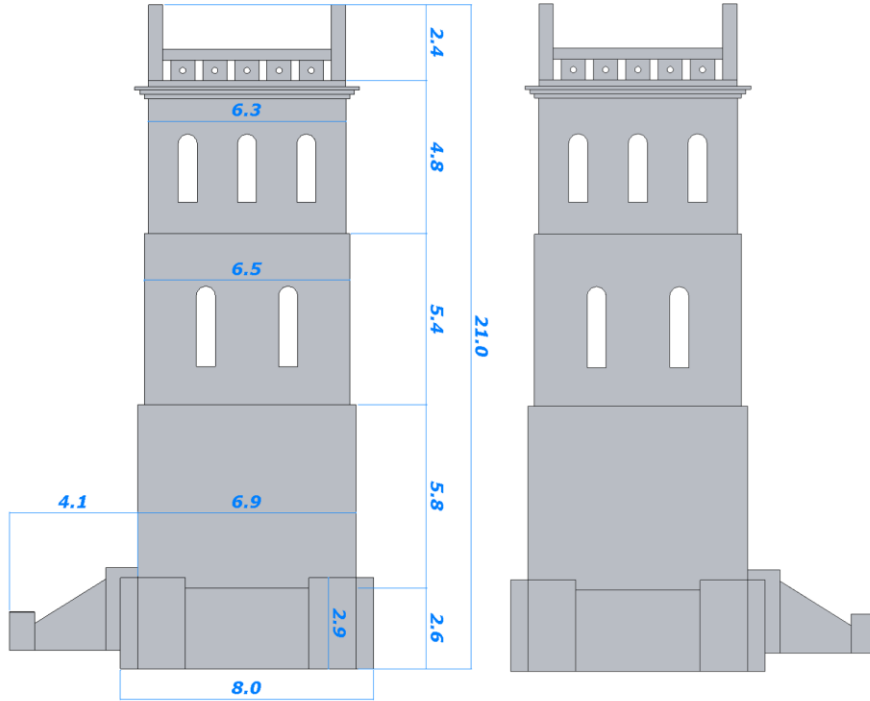

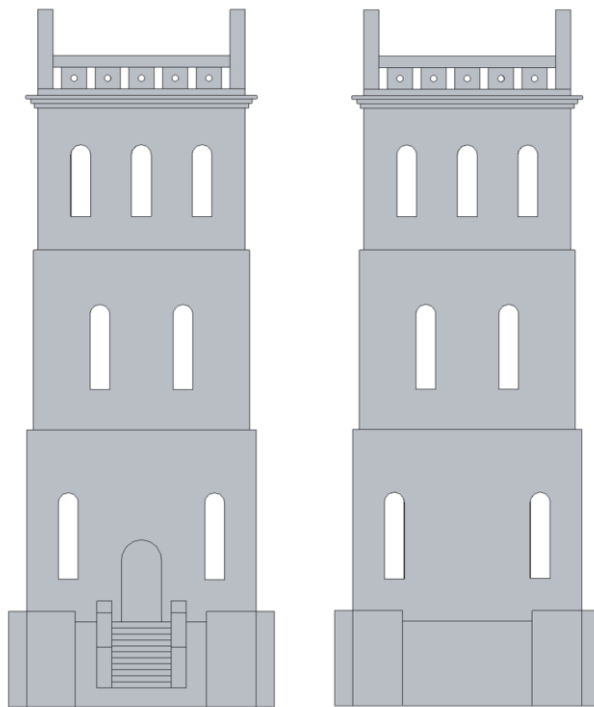*Figure 23 Revit 3D model east and west elevation*

Figure 24 Revit 3D model north and south elevation

Chapter 5: Numerical Modeling

5.1 Continuum Macro-Modeling

The macro-modeling of masonry structures is as mentioned in chapter 2 a modeling method for where the FE models are modeled with no distinction between the mortar and the brick units. As the modeling does not distinguish between the two elements, it is shown that this method of modeling is not suitable for smaller masonry structures or where the masonry units are too large [34].

The mesh does not correspond to the actual brick layout and thus it not a good method for simulation of small structures. The method will however be able to predict and simulate global behavior of structures, with a limited amount of computer effort comparted to a micromodel [35].

The FEM model that is to be modeled in continuum requires the equivalent material to be adequate when it comes to the physical-mechanical parameters, as it is going to represent the whole masonry material. Thus, the material properties chosen to characterize an averaged value of the masonry properties, must consider both the brick and mortar properties. As the intention with this thesis is to perform a modal analysis and not analyze local behavior the author has decided to proceed with a macro model of the tower.

5.2 Software and Import

The software that has been used in the FE modelling is Diana FEA. The software provides various analysis types for different kinds of structure and loading conditions [2].

Integrated into the software is the support for IFC, however the STEP file format allows for more options when import, such as adjusting the tolerances for import. The exported IFC file from Revit was exported with high detail and then converted into a STEP file with the free software CAD Exchanger [53]. Figure 25 shows how the procedure was performed.
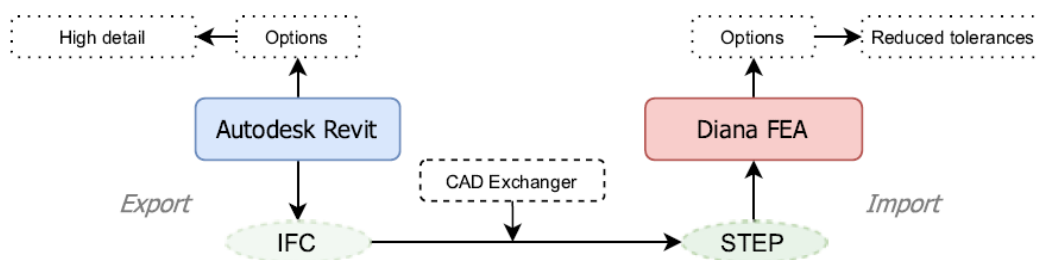

Figure 25 Procedure Revit to Diana FEA

The exported IFC model from the geometry modelling is easily imported into Diana FEA with the integrated support of STEP import. The results of the import into the FEA software is a model with no properties, leaving a blank canvas to work with in order to define all the needed parameters.

5.3 Computational Modeling

As the geometry is set, the Diana FEA software was not used to change or modify the geometry of the Slottsfjell tower in any way. Therefore, as explained in chapter 2, closing out 1 of the 4 steps of the computational modeling using FEM as shown in figure 26:
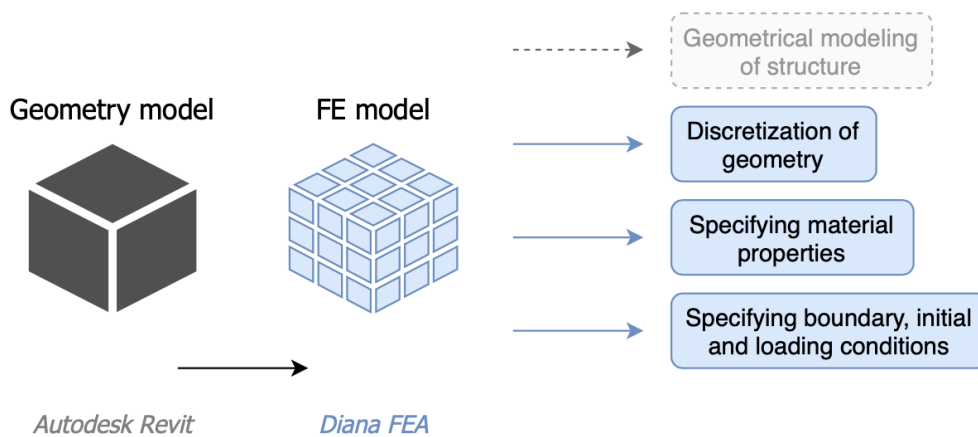
Figure 26 Approach for FE modelling

There is no specific order in which the above-mentioned steps should be completed, however all the steps need to be defined in order to perform the analysis and get the wanted results. Not specifying certain qualities of the FE model will give vastly different results, and it is therefore important to both specify all the point, but also give the individual points the accurate information (material properties, boundary conditions etc.).

Figure 27 shows the initial imported STEP model in Diana FEA (left) together with a modified model (right), where the geometrical modeling is finished. The imported model seemed somewhat distorted/irregular by the look of the lines of the initial imported step file. This could however be fixed, and the model could be "cleaned" with the integrated tools in the Diana software.

These tools can be found under "properties" and are:
- remove small entities
- clean shape
- optimize shape

The values used in the optimizing and cleaning of the model are the default values, which are given as a tolerance of $1*10^{-5}$ m.

The resulting model is much cleaner looking, as these tools will remove smaller entities as defined by the user. In addition to this, the tools will reshape any angular lines which have a deviation more than wanted (user defined) including overall optimization of the model for an easier and more optimal analysis.
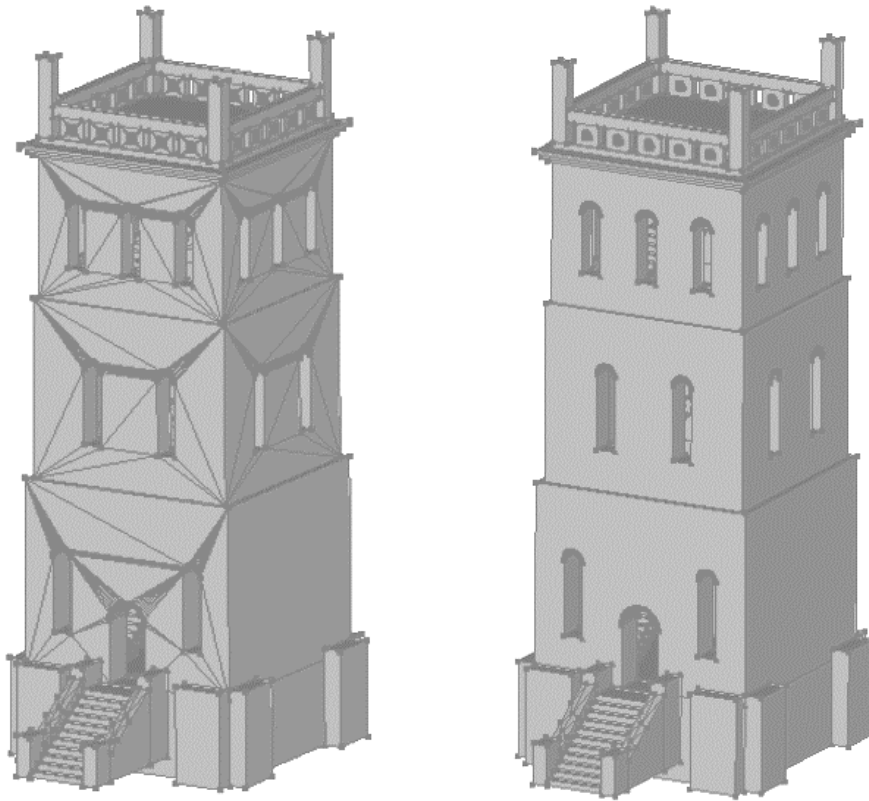

Figure 27 STEP model in Diana FEA

To get an accurate model, there are certain areas of inaccuracy that need to be eliminated. Main sources of error in FEA can be defined in three categories [54]:

- User inaccuracy
- Modeling inaccuracy
- Discretization inaccuracy

These three categories were important to evaluate while modeling the structure and will in general impact the wanted level of accuracy of the model. Therefore, a lot of time was used on both the geometrical modeling, but also the FEA analysis parameters to eliminate unwanted errors and in return reduce the imprecision of the results.
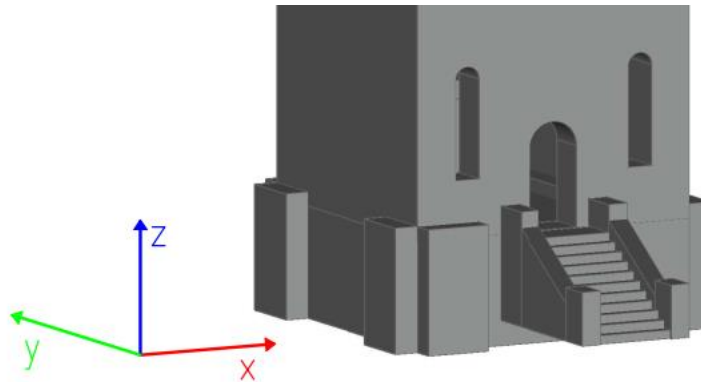
5.3.1 Axis Definition

Figure 28 Global axis system in Diana FEA

Figure 28 shows the axis in the model, where x-x and y-y are axis in the plane and the z-z axis is out of plane. This axis data is also used presenting the corresponding results.

5.3.2 Discretization

The meshing of the geometry allows for a finite number of elements to be analyzed which divides the geometry into a patch of smaller portions. The more elements the model is divided into, the more accurate the analysis will be. On the other side, it will also increase the overall time of calculations and overall need for computational power. Regarding this, a balance of both computing time and accuracy needs to be addresses in each individual FE model.

For the model at hand, an initial size of the mesh of 0,2m was compared to 0,15m, which results in cubes of 0,008m^3 and 0.003375m^3 respectively, where the smaller mesh gives around 2,4 times more elements. The results of an arbitrary modal analysis performed showed around 1 % deviation of the results when comparing the mesh size. On that basis an initial element size of 0.2m was defined and kept. Table 3 shows the element size and the corresponding mesh type the FE model was split into. The resulting model after the discretization is shown in figure 29.

Table 3 Mesh data Diana

Type	Value
Mesh	8 node hexa/quad (with adaptive element size)
Size	0.2m

When performing the discretization, the software had difficulties in the meshing of the stairs. Because of the stairs contribution to the overall stiffness of the structure and an evaluation of the difficulties in getting the meshing right in the quite complex geometry of the stars, it was decided to remove them altogether in the initial model of the tower. Also adding the fact that the internal stairs are

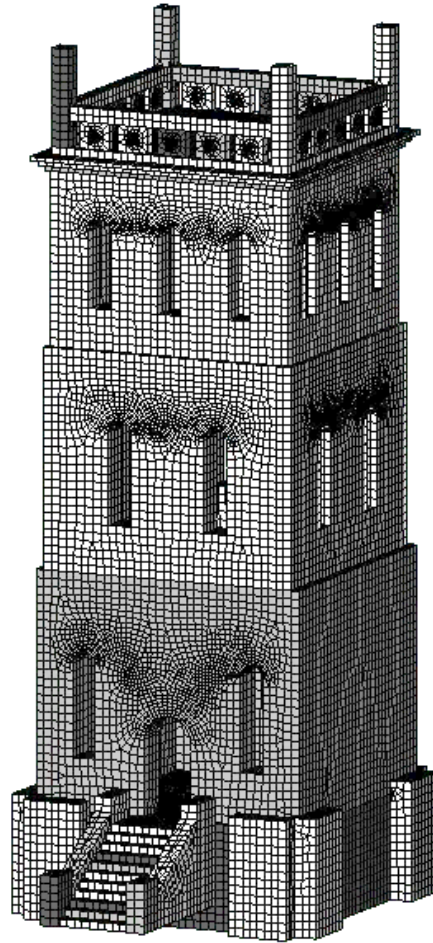nonstructural elements of the structure, contributed to removing them for simplification.

Figure 29 Discretized FE model in Diana FEA

Furthermore, as seen in the figure 29, an adaptive mesh size was used. This option allows the software to adapt the element size of the resulting mesh in openings and more complex geometry, allowing for a better discretization of the masses and in turn giving an overall better analysis.

The external stairs and the base of the tower had a bigger mesh than the overall structure, where the size of the mesh was set at 0.3-0.35 m appose to 0.2m. This was done to prevent internal errors caused by the creation of mesh sizes with zero volume. By defining a manual element size and with trial and error it was possible to find the ideal element size that did not cause this.

5.3.3 Material Properties

The material properties of the discretised geometry are defined for the homogeneous masonry material as shown in figure 30. Where the values for the

equivalent material used in the FE model are isotropic, meaning they are equal in x, y and z direction. While the homogeneous definition of the material will allow for a simplified FE analysis, it is also not suitable for detailed stress analysis, as explained in further detail in chapter 2 [55]. In our case the equivalent material will be enough to perform a global analysis of the tower, such as the intended modal analysis.
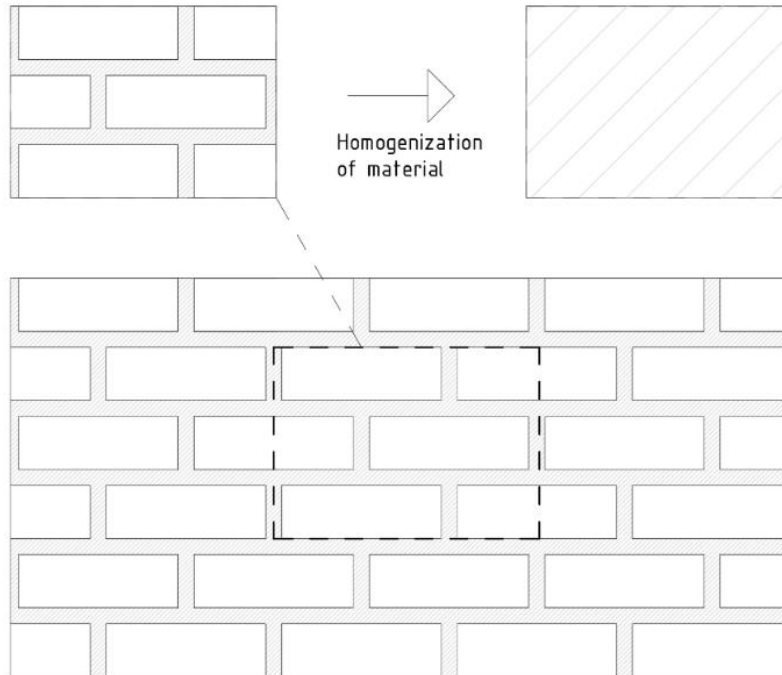

Figure 30 Homogenization of masonry

The natural stone type present in the tower is Tonsbergite, which is a variant of the Norwegian igneous rock Larvikite, where the main differences are the color and feldspar minerals. [56] The Larvikite rock is related and classified as a variant of monzonite rock. [57] Compared to granites, which is more broadly know, the monzonite has a lower percentage of quartz.

Because of the varying results of many experimental tests performed on masonry stone structures, the mechanical properties rarely have a fixed value. In addition, the initial properties chosen for the FE model will be adjusted according to the ambient vibrating data, therefore the actual initial value does not need to be completely accurate. Moreover, the properties chosen do not need to be explicitly correlated to the natural stone present in the masonry of the Slottsfjell tower, as of this.

Masonry type	Masonry properties					
	f_m (MPa)	τ_0 (MPa)	E (MPa)	G (MPa)	ρ (kN/m³)	f_t (MPa)
Irregular stone masonry	1.0–1.8	0.020–0.032	690–1050	230–350	19	0.030–0.048
Multileaf masonry with thin outer layers of rough-worked ashlars and rubble core	2.0–3.0	0.035–0.051	1020–1440	340–480	20	0.520–0.076
Rough-cut stone masonry with good texture	2.6–3.8	0.056–0.074	1500–1980	500–660	21	0.084–0.111
Soft-stone ashlar masonry	1.4–2.4	0.028–0.042	900–1260	300–420	16	0.042–0.063
Stonework with squared blocks	6.0–8.0	0.090–0.120	2400–3200	780–940	22	0.135–0.180
Brickwork with solid units and lime mortar	2.4–4.0	0.060–0.092	1200–1800	400–600	18	0.090–0.138

Figure 31 Existing masonry properties [30]

The initial mechanical properties used for the natural stone present in the tower is based on the properties of stonework with squared blocks, as presented in figure 31, marked in yellow [30]. The figure presents the density of the material as well. In addition, there is also concrete present in the tower, where the floors are of concrete. The properties are here chosen based on the assumed quality of the concrete, and standardized values for concrete given in the Diana software for concrete grade C35.

Table 4 Material properties masonry - linear

Property	Masonry
E-modulus	2.4 GPa
Poisson's modulus (v)	0.2
Density	2240 kg/m³

Table 4 presents the initial input used for the material properties for the masonry in the model.

For the initial value of the material properties an isotropic material model is used. In this case Diana automatically defined the G modulus according to the relation between the modulus of elasticity (E) and Poisson's modulus (v), as presented in the formula under.

$$G = \frac{E}{2(1+v)}$$
 (9)

5.3.4 Boundary, Initial and Loading Conditions

For the loading, no external loads where added. The only loads acting on the structure is the self-weight as defined earlier through the density of the material. The self-weight is defined in the model through a global load acting on the whole structure.

For the boundary conditions applied to the structure, two different alternatives were modelled in order to verify the difference the separate approaches would result in. One model is made with the implementation of SSI and one without, this is also explained more in depth in chapter 2.

The first model is modelled as a simplified cantilever with fixed translation in all directions. This is done with simply constraining the bottom of the tower directly as indicated with the red triangles. The constraints of the tower are defined through fixing of the 3 degrees of freedom (3 translations), applied to movement in the fixed point of the tower.

On the other hand, the second model was modelled with a full soil-structure interaction. The method implemented is only going to be explained briefly in this chapter, for a detailed explanation and step by step tutorial of the procedure of the modeling, the following tutorial is available [58].

Table 5 presents the values used for the different properties in the SSI implementation in Diana.

Table 5 Initial input data SSI

Property	Soil	Interface
E-modulus	160 MPa	
Poisson's ratio	0.3	
Density	2200 kg/m³	
Normal stiffness modulus-z		1 GPa
Shear stiffness modulus x/y		10 MPa

The SSI interaction, with the corresponding modelled foundation set on the structure is present in figure 32, where the interface between the soil and the structure is given by a no tension constant shear stiffness for the interface material. Details of the implementation can be found in the tutorial referred to previously and in chapter 2.
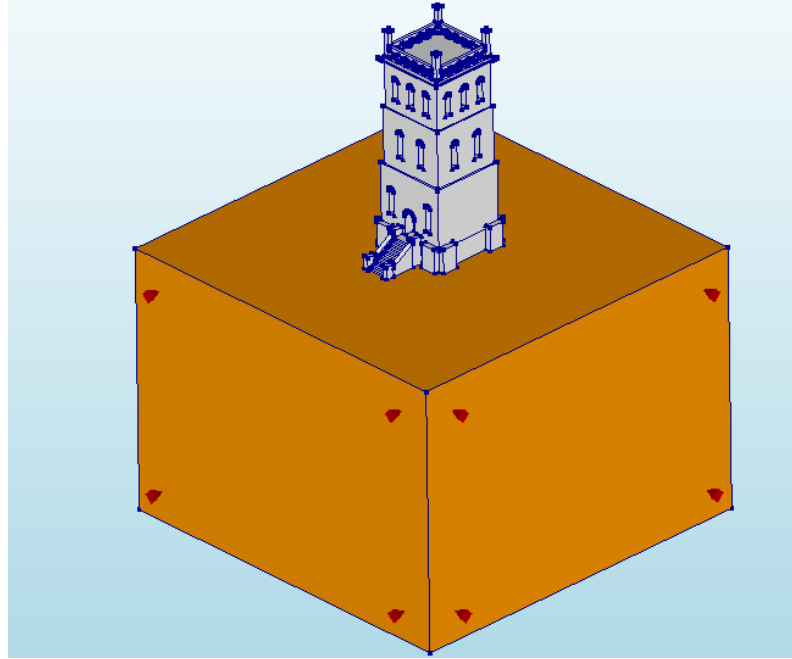
_____

Figure 32 SSI supports of model in Diana FEA

As the tower itself has the lower part inside the soil, this was modelled as seen in figure 33, where the shape of the tower was "cut" out of the soil. The model was then placed inside the cut soil.
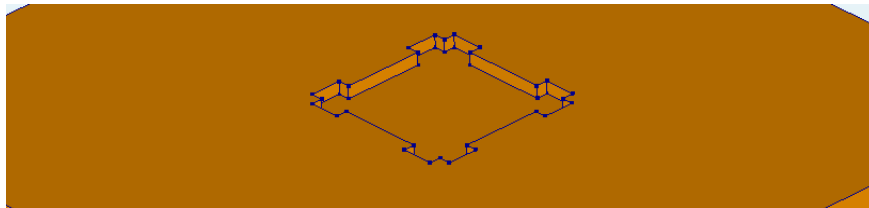

Figure 33 SSI soil of model in Diana FEA

The interface is defined for the part of the structure that is in contact with the soil, as highlighted in figure 34.
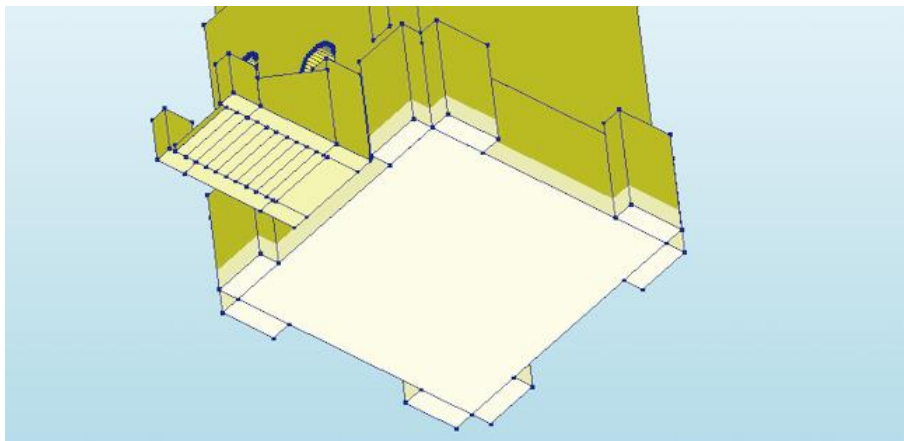

Figure 34 SSI interface of model in Diana FEA

The simplified approach with constraints directly on the structure is seen in figure 35. The supports are placed on the bottom of the structure, which represents the part of the tower that is placed inside the soil. This simplified approach is also mentioned in chapter 2.

To achieve this placement of the constraints the bottom part of the tower was split into another part, and the supports where then added on the surface of the new part.
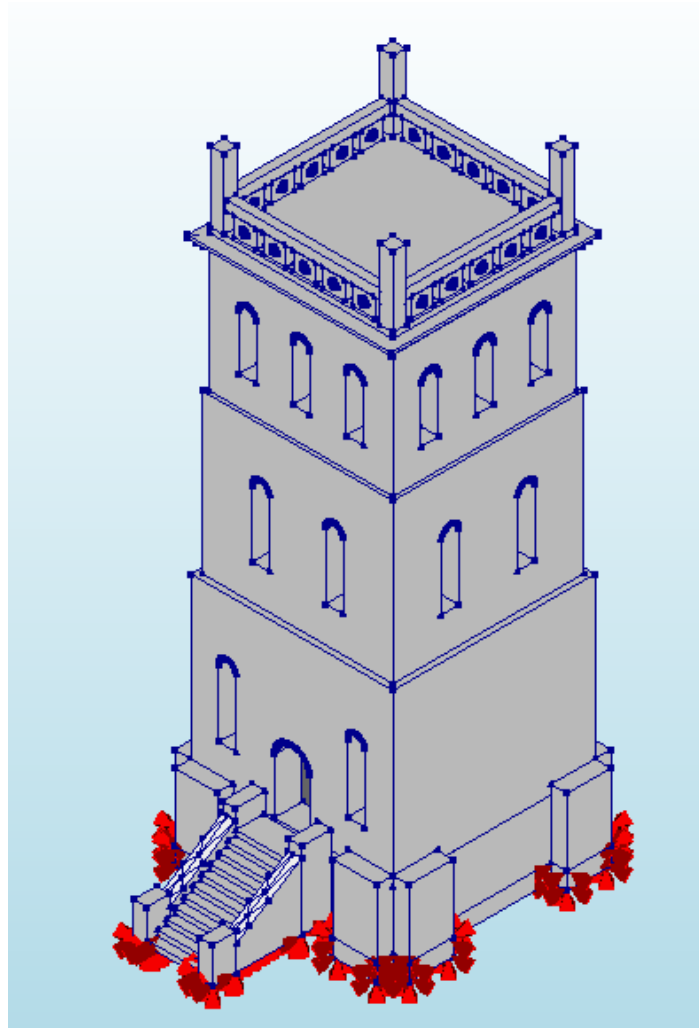
Figure 35 Simplified supports of model in Diana FEA

5.4 Modal Analysis

After defining the four steps of the computational modeling, which are the geometrical modeling, the meshing, definition of the material properties and finally the definition of the loading and boundary conditions, the model is ready for analysis.

The Diana FEA software allows for performing several different analyzes, in this case the one that is of our interest is modal analysis which is defined in Diana as structural eigenvalue. The first modes are the most critical and therefore the most interesting in correlation to acquired data from the AVT. These modes are related to the lowest frequencies, and therefore also the most attractive when considering resonance and structural movement.
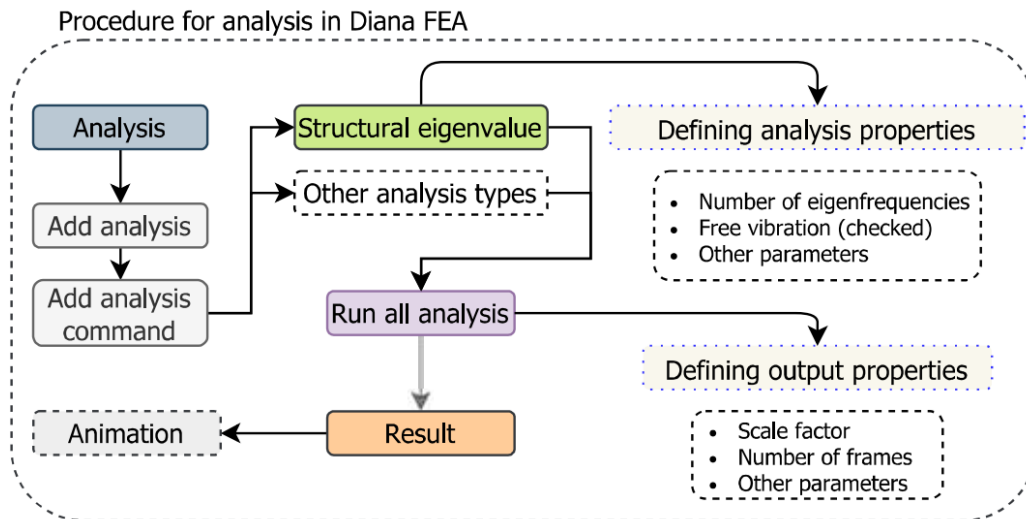
Figure 36 Analysis procedure in Diana FEA

The procedure in adding and performing modal analysis and other types of analysis is given in figure 36. After adding a certain analysis with the wanted parameters, it can be saved for later use. This is especially useful when the analysis is to be performed several times with change in geometry, material properties and other properties in between different analysis, which is the case here.

5.4.1 Results of Initial Modal Analysis

The results of the initial modal analysis, where the mode shapes are given together with the frequency, are presented under in the next paragraphs.

Figure 37 shows the first mode for the model with SSI and figure 38 shows the first mode of the tower without SSI implementation.
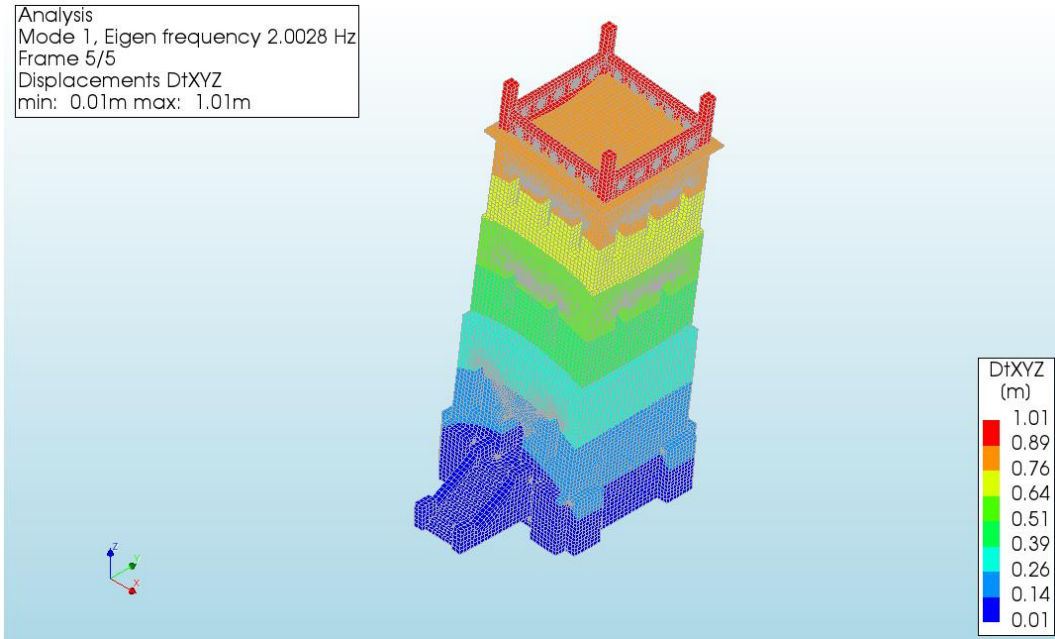
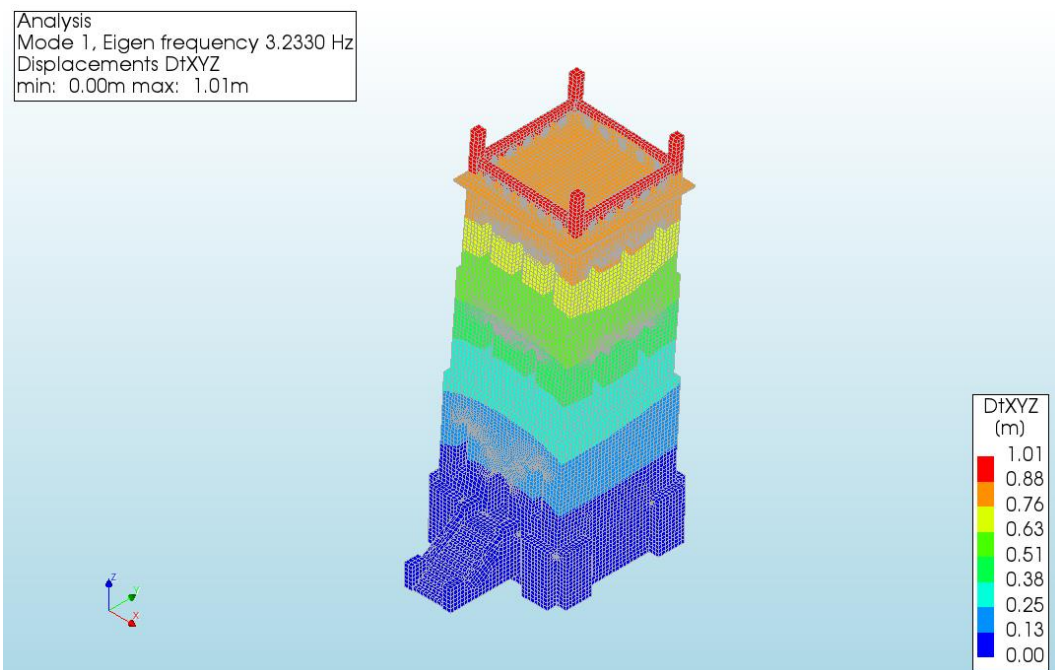*Figure 37 Results mode 1 - model with SSI*

Figure 38 Results mode 1 - model without SSI

Table 6 Numerical Modal Analysis Results

Approach	Property	Mode 1	Mode 2	Mode 3	Mode 4	Mode 5
Without SSI	f (Hz)	3.23	3.37	7.31	8.91	9.88
SSI	f (Hz)	2.00	2.22	5.11	5.11	5.48

47

_____

Table 6 shows the result of the first 5 modes with figures 39 and 40 showing the deformed shapes of the model without SSI and the model with the SSI implementation.
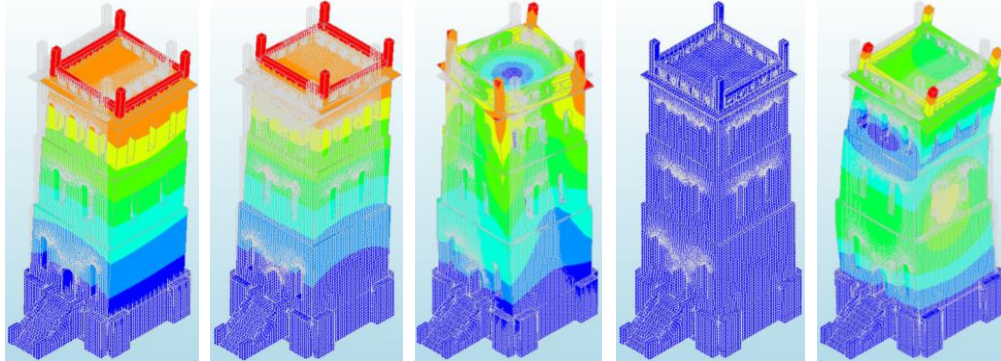
Figure 39 First 5 modes for model without SSI
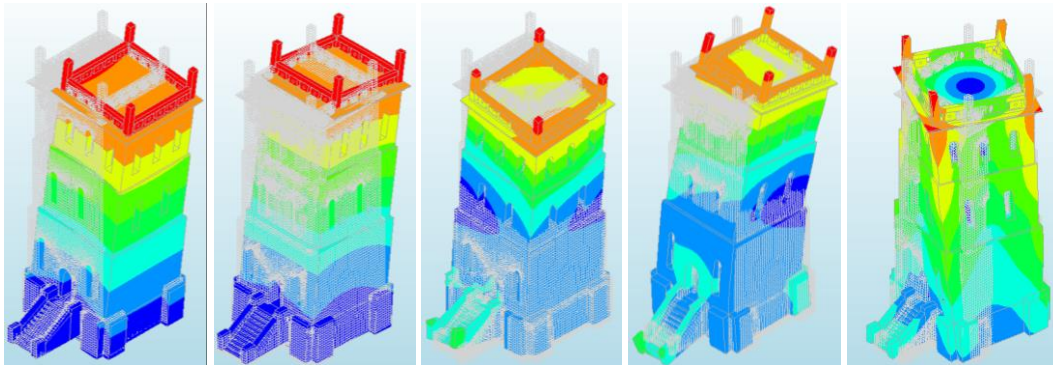
Figure 40 First 5 modes for model with SSI

When looking at the two different cases, we see quite a big change in the frequencies. The approach taken in the support; without and with SSI, shows that the effect of the SSI is making a big impact on the output of the modal analysis. One of the modes in the model without SSI shows no global movement of the tower and is therefore a local mode shape.

Table 7 Comparison SSI and without SSI results

Approach	Property	Mode 1	Mode 2	Mode 3	Mode 4	Mode 5
SSI/without SSI	%	62	66	70	57	55

Table 7 presents the percentage of the model without SSI to the SSI method with respect to the natural frequencies of the first 5 modes. As seen in the table and the results of the modal analysis performed on the SSI and simplified model, we can take the following conclusions: The natural frequencies extracted from the modal analysis of the SSI model shows that the frequencies are around half to two-thirds of that of the model without the SSI implementation, when looking at the first five modes.

At this stage, the actual ambient vibration data is not available, therefore both models are relevant. When the ambient vibration data is available and the dynamic characteristic are extracted, then it is possible to know which model is most suitable to proceed with. With the proceeding of one of the models, there are then possibilities to tweak the model with the material properties, as the discretization, the supports and the geometry is fixed from the previous works performed on the models.

5.5 Gravitation Analysis

In this section a basic linear static analysis is performed on both the models, where the displacements of the models impacted by the self-weight are presented. This is done to verify that the load distribution is as expected. No other load other than the self-weight of the geometry is added in the model. The displacements are not actually showing real life use, as there will be static live loads such as, snow, furniture, and dynamic loads such as wind and human walking. Figure 41 and 42 shows the results of the analysis.
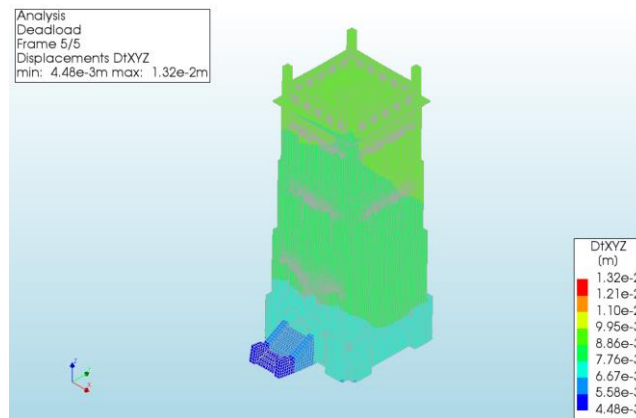
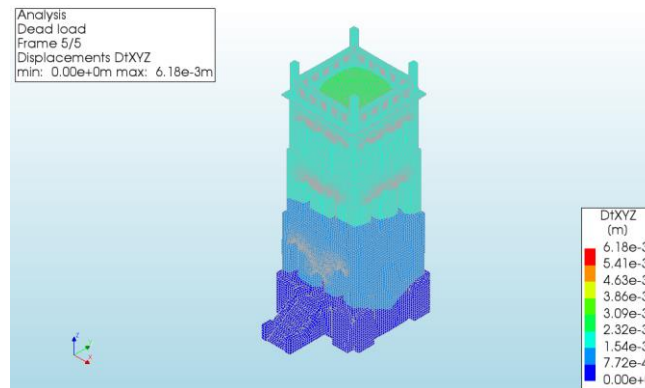*Figure 41 Results displacement - model with SSI*

Figure 42 Results displacement - model without SSI

The results of the analysis are as expected and shows that the load distribution is good. Therefore, both models can be used to proceed with.

Chapter 6: Ambient Vibration Testing

6.1 Overview

As the OMA is dependent on that the acquired measurement data is of good quality, it is very important for the AVT to be done in such a manner that allows for this data to be good enough. Therefore the measurements should: a) be carefully planned and executed and b) good quality signals are captured at each test setup [7].

6.2 Accelerometers

6.2.1 Placement and Number of Sensors

The placement and numbering of the accelerometers used is connected to the risk of placing them in nodes, which will not be able to provide the modal properties. In that case, causing the measurement to be redone because there is not a sufficient number of sensors. We know that in this structure there will not be a node in one of the top corners for any of the modes, and therefore it is a good position for sensors.

The number of sensors used is related to the risk of not achieving the wanted results if they do not work as intended. Several research cases used four accelerometers with success, [5, 29] in addition to available literature that states that a minimum of four sensors should be used [7]. While other studies have used more than four sensors for a similar structure sizes [25].

The number of sensors can also be determined with the following questioning, what is the rank of the problem? [7] This strategy considers the estimated spectral density matrix, while also considering noise sources and from there choosing the minimum number of sensors to be used. The matrix is defined as the number of modes that are contributing to the response of a frequency band. Since the matrix will also take into account the modes and the noise sources then the rank of the problem will be defined as modes + noise sources, thus implying that the minimum number of sensors should be the same as the rank of the problem. Other strategies to estimate the number and placement of the sensors are FE simulations [7, 59].

When it comes to the positioning of the sensors, there are a lot of different methods available. As stated in [60] almost all papers related to experiment design are modelled as statistically independent random variables, which is not the case with engineering structures. The paper however proposes an experiment design method, based on a preposterous analysis, taking the costs of the experiment into account. Other papers also estimate the best placement based on a modeled FEM model

Studies carried out to achieve an optimal placement of sensors uses the modal assurance criterion (MAC) to provide the statistical correlation between the observations between the numerical model and experimental measurement. The MAC is defined under and indicates how good the correlation between the two observations are, given as a number between 0 (no correlation) and 1 (good correlation) [61].

$$\frac{|\{\Psi_A\}^T * \{\Psi_X\}|^2}{(\{\Psi_A\}^T * \{\Psi_A\}) * (\{\Psi_X\}^T * \{\Psi_X\})} \tag{10}$$

where, Ψ_A and Ψ_X indicates the eigenvector for the complex damped mode of vibration for the analytical and experimental results.

The correlation of the results from the numerical model and experimental measurement is given as a matrix, which has been implemented in different studies in order to estimate the optimal sensor placement [62, 63].

As a summary a reasonable and cost-effective way of determining the positioning of sensors is shown to be a good distribution of them on the structure [7, 60]. Also, the risk of the sensors simply failing to read the vibrations because of hardware or software related reasons emphasises the idea of using more sensors than needed, while keeping the total amount low, both to reduce cost and needed computer power [62].

6.2.2 Duration

The total duration of the ambient vibration measurement should not exceed 3 hours, if not especially necessary [7]. Studies show that the time window for the measurements should be between 1000 and 2000 times the period of the structure's fundamental natural vibration [64]. Furthermore, the estimation of the natural frequencies of a given structure can be done with the use of national code equations as presented in [65]. According to the mentioned paper the ASCE 07-16 (2017) [66] provides the following formula of the estimation of the natural frequency:

$$f(H) = \frac{1}{0.0488H^{0.75}} \tag{11}$$

Whereas the Italian NTC-2008 (2008) [67] provides the following formula for the estimation of the natural frequency:

$$f(H) = \frac{1}{0.05H^{0.75}} \tag{12}$$

In addition, other estimates are also given in the Spanish Design Code NSCE-2002 (2002), however these will not be evaluated in this case [65]. Considering the equations given in ASCE 07-16 (2017) and NTC-2008 (2008) from the above-mentioned paper, in addition to the measurement interval discussed above, we get the following result:

Table 8 Estimation Time Interval for Vibration Testing

H = 17 m	Estimated natural frequency	Estimated period	Time interval (s)	
		1/f	x1000	x2000
ASCE 07-16 (2017)	f(H) = 2.4476	0.409	409	818
NTC-2008 (2008)	f(H) = 2.3889	0.419	419	838

As seen in table 8 the time interval should be somewhere in between 419 and 838 second in order to obtain accurate estimates of the modal parameters.

6.2.3 Specifications

All the specifications of the accelerometers used in this study are given in the appendix A [68].

6.2.4 Software

The software used for processing the raw data of the AVT is a software provided by supplier of the sensors. The software is a graphical user interface inside of MATLAB [69], called *Unquake Suite [68].* Appendix C shows details and an overview of the interface with the available features.

6.3 Initial Execution of AVT

The initial execution of the AVT was performed on a windy day, with desirable conditions to achieve good readings from the sensors. A total of 7 triaxial sensors where used in the AVT as presented in figure 43. The sensors were placed with one in each floor, whereas the 3rd and 4th level had two each. This includes one sensor in the basement of the tower.
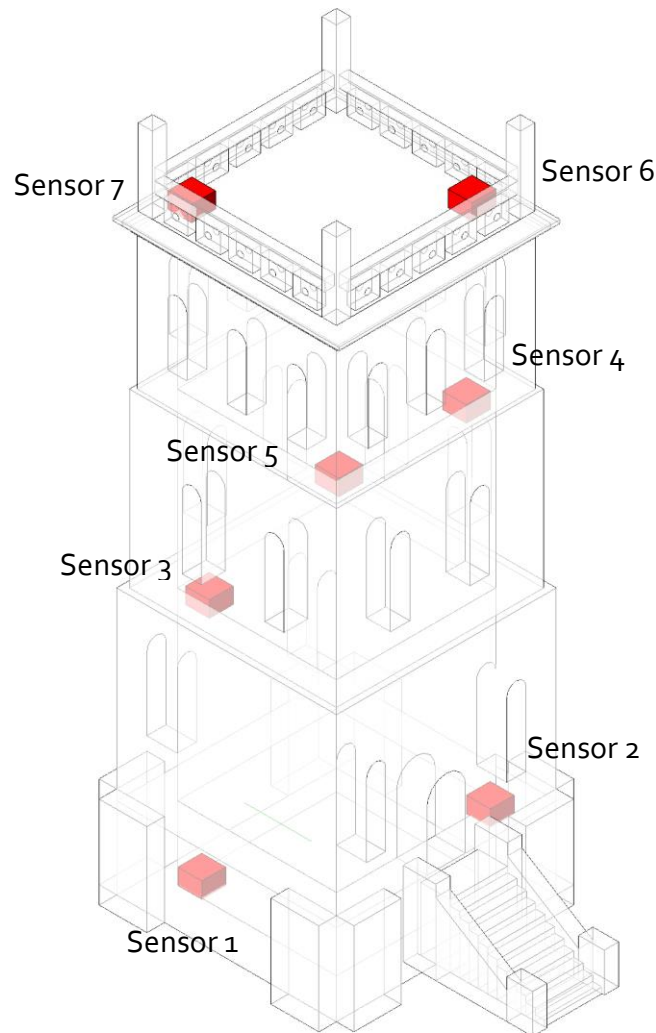
Figure 43 Sensor placement 3D view – initial reading

Each of the sensors where connected to a datalogger, as presented in figure 44. The dataloggers where then connected to a GPS antenna and plugged into power. This setup was the same for all the 7 sensors in each floor. In order to prevent unwanted movement in the sensors, the magnet of the sensor was placed on a thin steel plate over the magnet, this steel plate was then glued to the ground with epoxy glue to secure it for unwanted movement in the sensors.

Figure 44 Sensor and datalogger - initial testing

The data acquired from the AVT was extracted from the SD cards of each of the dataloggers. For practical simplification, an interval of 180 minutes was used for the reading of the initial AVT.

6.3.1 Results and Discussion

Figure 45 shows the acceleration in of the sensors used in the AVT, where the acceleration is given for the x, y and z direction. In addition, too this the figure also shows the GPS data, which is used for the synchronization of all the sensors in-between each other.

After processing the data through the software mentioned earlier with the use of the FFT, we get the reading in the frequency domain as seen in figure 46. The results of the initial readings showed too noisy data, which was too difficult to assess. As seen in the figure 46 for one of the sensors in the lower floors, there are no distinct peaks in the amplitude of any of the frequencies, it was therefore very difficult to assess the results. The processing of the data showed that the lower floors had very low readings on the sensors, as also visible from the figure under. In order to get more and better readings, the placement of the sensors were therefore changed in the second AVT.

After being in contact with the supplier of the sensors, it was advised to redo the AVT with much longer time intervals, lasting longer than the initial one. The range which was suggested was at least from 2 to 5 days, in order to get good reading and reduce unwanted noise.
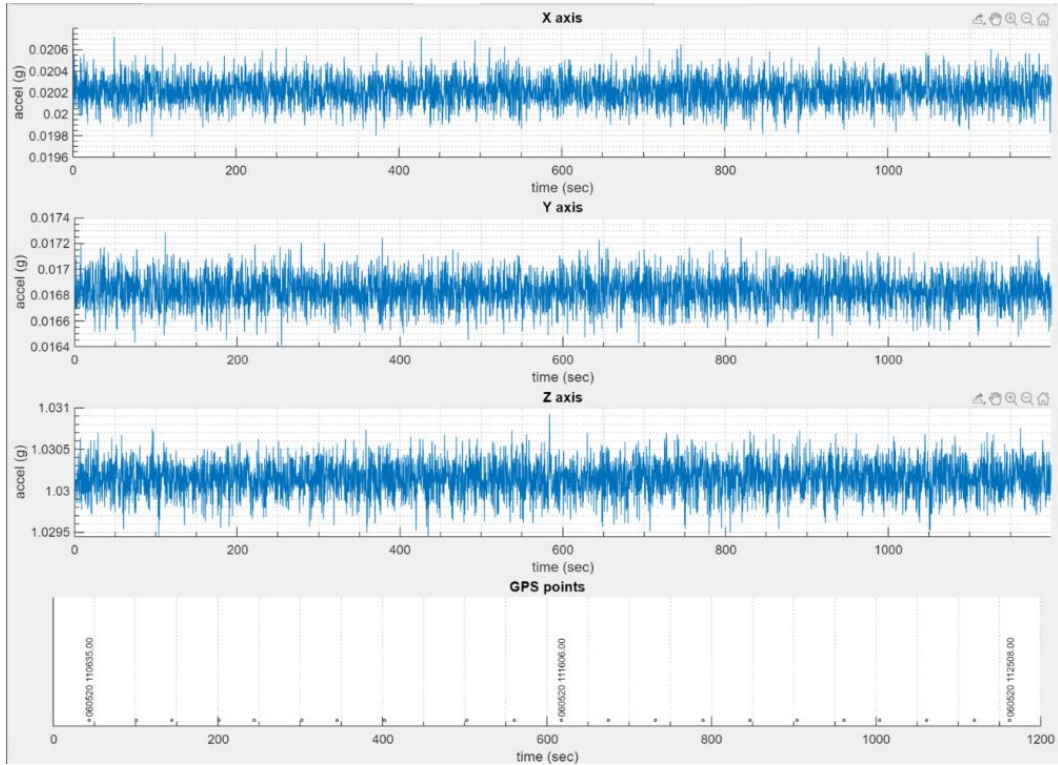
Figure 45 Sensor acceleration graph
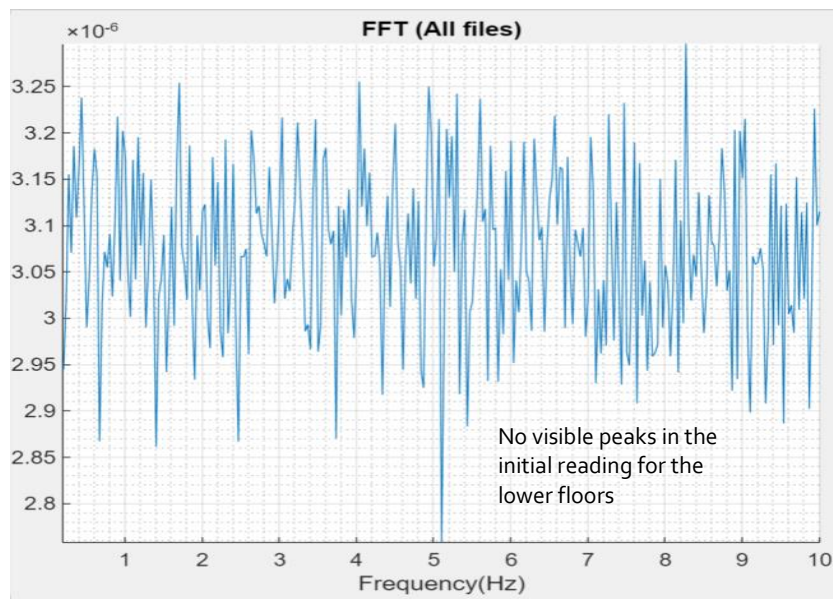
Figure 46 Result first reading – lower floor

_____

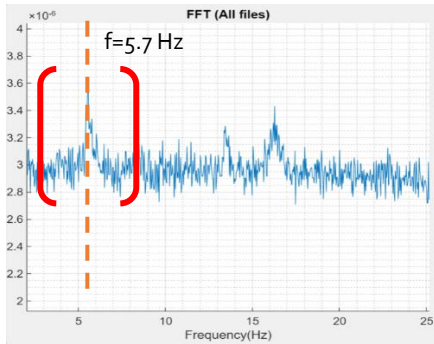<u>**Initial reading**</u>

x-direction	y-direction

Sensor 3

Figure 47 Sensor 3 x-direction - initial reading
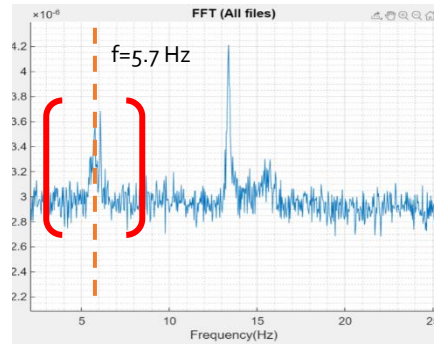
Figure 48 Sensor 3 y-direction - initial reading
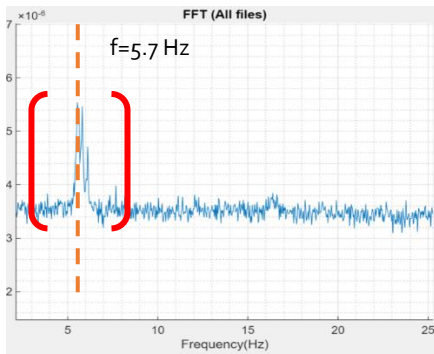
Sensor 6

Figure 49 Sensor 6 x-direction - initial reading
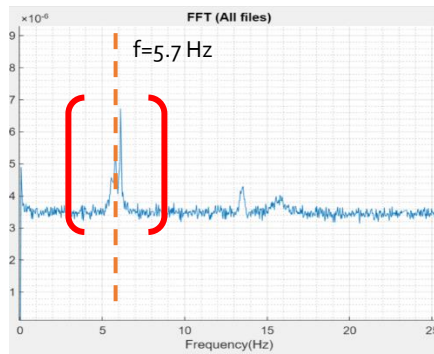
Figure 50 Sensor 6 y-direction - initial reading

While the measurement was indeed noisy, there were some peaks in the graphs. This can be seen in the figures above, where the measurements of two of the sensors are presented. Both for the 3rd and 6th sensors there is visible peaks, however they are not consistent in all the measurements and therefore not good to proceed with.

The full set of results from the first reading is available in Appendix B. For the initial reading the results for sensor 1 and 2, placed in the lower floors are not presented due to too noisy measurements.

6.4 Second Execution of AVT

For the second execution there were placed a total of 6 triaxial accelerometer on the tower for the ambient vibration measurement. Figure 51 shows the position of the them in a 3D view of the tower. All the sensors were placed on the ground with the x and y axis on the horizontal plane, while the z-axis was working vertically upwards, which was also done in the first reading. The sensors are marked with the x-axis (blue) and the y-axis (green) to indicate the local axis for each of the sensors.

As mention earlier, from the results of the first reading there were only good readings from the sensors placed in the higher levels. In addition, we know that the tower will have more movement in the higher levels than the lower, therefore the sensors were only placed in the 3 upper levels for the second AVT. One sensor from the first reading was removed due to a faulty cable.
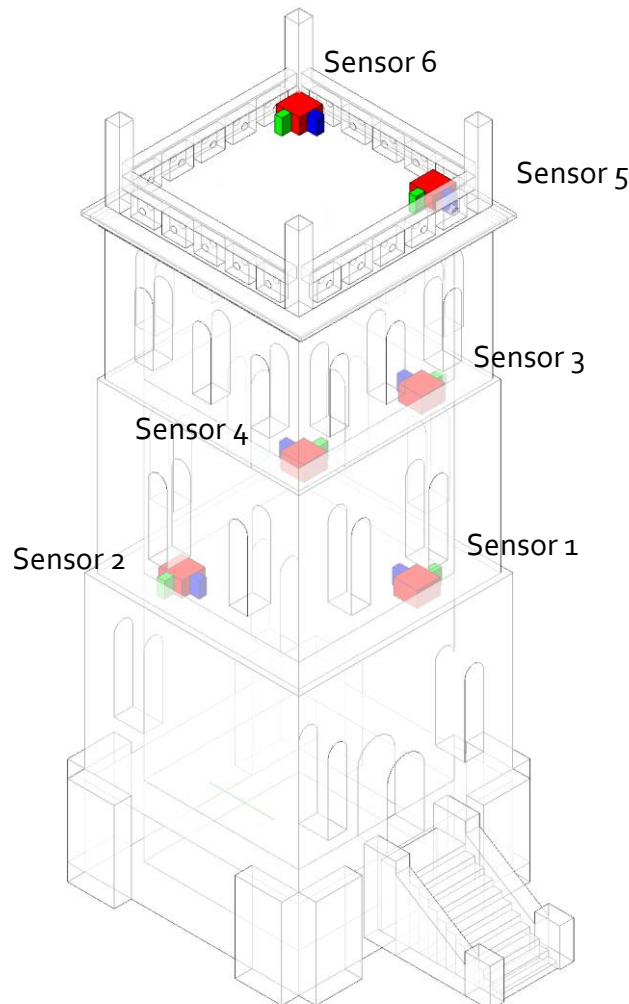
Figure 51 Sensor placement 3D view – second reading

The Slottsfjell tower can be qualified as a "box-type" structure, the main movements that are of interest are the horizontal in each direction in addition to torsion. The vertical deflection can be neglected in this case [7]. On the basis of the above mentioned the deformation in the z-axis is not of interest in this case. As these sensors have more sensitivity in the x and y direction, this placement is good.

Figure 52 Sensor, datalogger 3rd floor - second reading

Figure 53 Sensor and datalogger roof - second reading

Figure 52 and 53 shows one sensor placed on the 3rd floor and on the roof level. The setup is the same as the initial AVT, where the sensors and GPS antenna is connected to the datalogger, which is in turn connected to power. The steel plate under the sensors are glued to the ground with epoxy glue to ensure no unwanted movement in the sensors, while the readings are done.

6.4.1 Results and Discussion

The raw data which was accumulated and saved on the dataloggers were processed in the same way as the first reading through the software in MATLAB. The figures under shows the results from several of the sensors in the second reading. As seen in the figures the first peak is visible around the frequency of 5.7 Hz, for both the accelerometer in x direction as well as the ones in the y-direction.
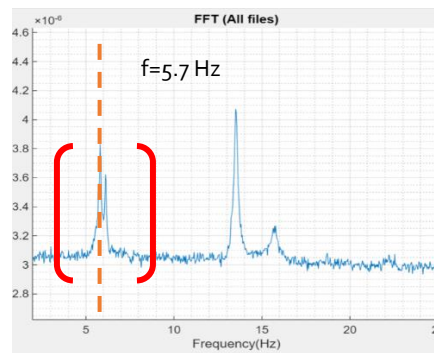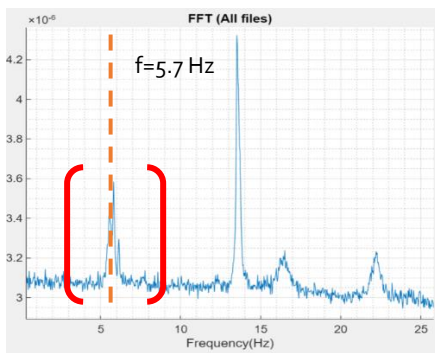
Second reading

x-direction	y-direction

Sensor 1

Figure 54 Sensor 1 x-direction - second reading

Figure 55 Sensor 1 y-direction - second reading
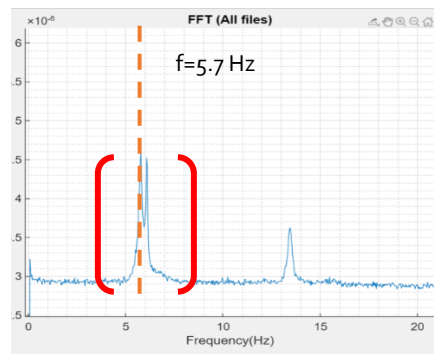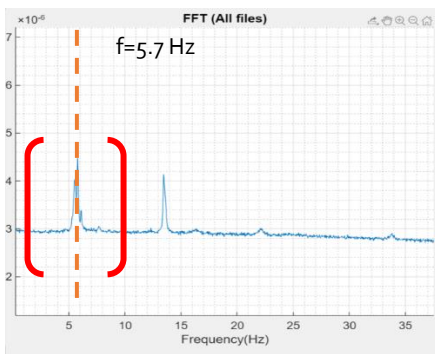
Sensor 3

Figure 56 Sensor 3 x-direction - second reading

Figure 57 Sensor 3 y-direction - second reading
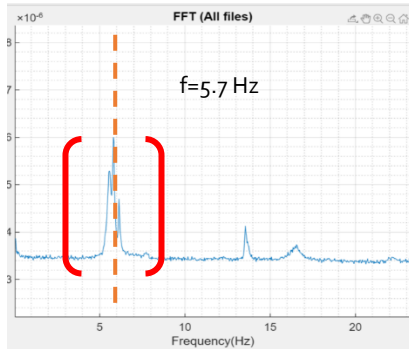
Sensor 6
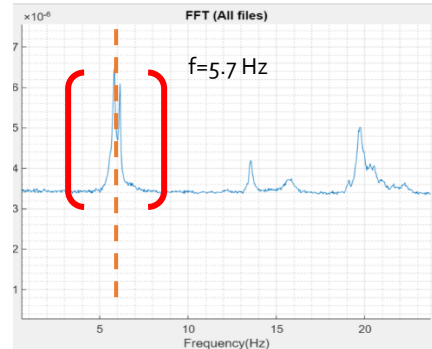
Figure 58 Sensor 6 x-direction - second reading   *Figure 59 Sensor 6 y-direction - second reading*

Based on the results from all the sensors, it was seen that this peak around 5.7 Hz was visible in all of them. By identifying this first peak, this frequency is considered the first natural frequency of the tower, and the numerical models would be adjusted according to this.

Postponing of the executing of the AVT did not allow for a long period of calibration for the numerical models, therefore the calibration did mainly only consist of changing material properties. There were no changes in the discretization, and or geometry of the models. The calibration process was performed on both the models; both with SSI and without SSI, for the first frequency.

Chapter 7: FE Model Calibration

7.1 Overview

From earlier, we have two different models of the tower, differentiated with the support's implementation. One model is modelled with traditional supports with restrains on the structure directly, whereas the second is modelled with the SSI. From the initial modal analysis performed of the two structures it was clear that the support implementation has a big impact on rigidity of the structure and thus the natural frequency of it.

The material properties on the masonry varies a lot and the initial values used were only used as a starting point for the calibration. Similar studies of OMA calibration with FE modelling of stone masonry structures used values for the E-modulus up to around 4500 Mpa [70]. While other papers states that the E-modulus can be bumped up to 11 Gpa [71].

We can expect that the tower has been retrofitted over the years, because of the tower's age. Therefore, the values of the E-modulus can in fact be even higher than that of the above-mentioned papers. These values have therefore not been limited for the calibration.

Another important aspect in the model is the stairs, several papers have looked at the effect the stairs have on a given structure on the seismic performance of it, and the effect is big [72, 73]. Because the stairs are not implemented in the numerical models, this gives room to increase the material properties of the masonry to compensate for the lack of stairs. Short amount of time prohibited the full implementation of the stairs into the numerical models.

The calibration of the models can be summarized into these steps:
- The geometry of the models will remain the same
- Boundary conditions will change to give better estimates, if necessary
- Different material models will be estimated, to find the best calibration
- Material properties will be adjusted to find the proper estimation

Because the results from the AVT and the initial values of the modal analysis are quite far of, only the first mode is going to be calibrated as mentioned earlier. For both the SSI model and the model without SSI the material models used in the calibrated models where changes from linear isotropic to linear orthotropic material model. The reason for this is that the orthotropic material models also allows for inputting the shear modulus (G), whereas the isotropic ones do not allow for this. The E-modulus for each direction was however kept the same, and not changed in different direction.

_____

7.2 SSI model Calibration

From earlier we have quite low results for the initial modal analysis performed on the SSI structure for the first natural frequency.

In order to increase the overall rigidity of the structure both the soil and the masonry properties were adjusted. In addition to this the interface of the SSI was also increased in order to increase the rigidity of the interaction and thus making the structure stiffer, corresponding to the results from the AVT. Table 10 presents the final properties in the SSI model after the calibration, as well as the results of the analysis in figure 60.

Table 9 Material properties SSI - final

Property	Masonry	Soil	Interface
E-modulus	11.2 GPa	6 GPa	
Poisson's ratio	0.2	0.25	
Shear modulus	3.8MPa		
Density	2000 kg/m^3	2000 kg/m^3	
Normal stiffness modulus-z			1000 GPa
Shear stiffness modulus x/y			1 TPa
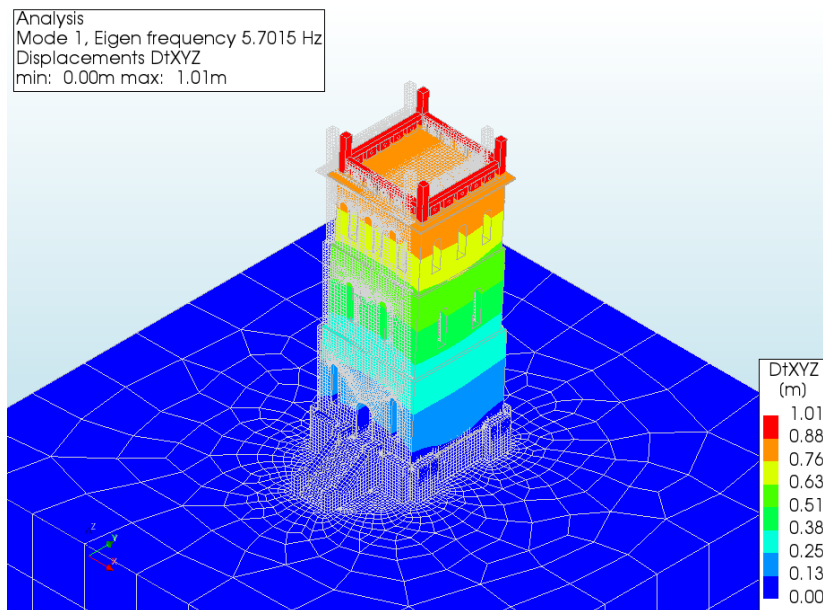
Figure 60 Mode 1 – calibrated model with SSI

7.3 Without SSI Model Calibration

Similarly, to the model with SSI, also the model without the implementation of SSI has a low frequency from the initial modal analysis.

Like the SSI model, also the model without SSI had the material properties increased. Compared to the SSI model, this one only had the masonry as the main tuning target, while the more complicated SSI model also had the soil and interface options. Table 12 presents the final material properties of the linear material model of the masonry in the model without SSI, as well as the results of the analysis in figure 61.

Table 10 Material properties without SSI - final

Property	Masonry
E-modulus	7,25 GPa
Poisson's ratio	0.2
Shear modulus	2.4MPa
Density	2000 kg/m^3
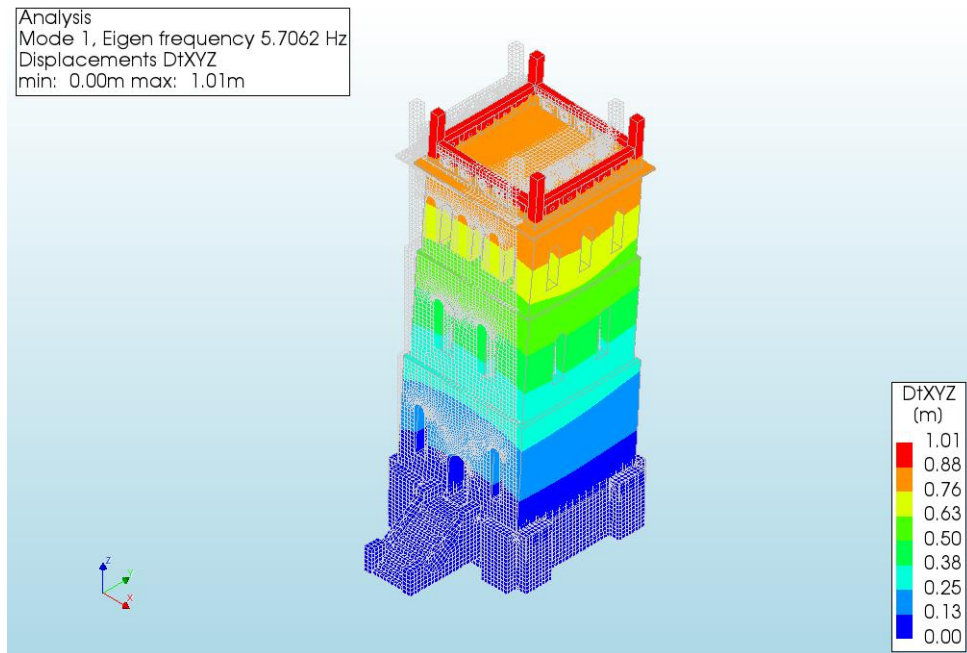
Figure 61 Mode 1 – calibrated model without SSI

7.4 Nonlinear Calibration

In addition to the simplified linear material properties, another model is made with the use of nonlinear material properties.

The material properties are inputted through the "total stain-based crack model" provided in Diana. Besides this material model, there are several different material models to choose from, however because the model is made up of 3D solids this material model is chosen. For example, the "engineering masonry model" is good when working with shell elements [74].

The final values used for the material properties for the nonlinear analysis are given in table 13.

Table 11 Material properties masonry nonlinear

Property	Without SSI	SSI
E-modulus	6.75 GPa	10.5 GPa
Poisson's ratio	0.2	
Density	2000 kg/m³	
Compressive strength	41 Mpa	
Tensile strength	0.9225 MPa	

For the relation of the compressive and tensile strength of the masonry the formula presented below, is considered. Where the tensile strength is given as 2.25 % of compressive. The compressive strength is based upon test result of strong stone masonry [71].

$$f_t = 0.0225 * f_m \qquad \textbf{(13)}$$

The nonlinear material model does not use orthotropic properties such as the linear material model. It rather uses the isotropic properties for the linear values. Therefore, the E-modulus for the nonlinear material model had to be reduced to reach the same frequency for the first mode as the linear orthotropic material model. The reduction was at 7 % and 6 % for the model without SSI and with SSI, respectively.

This reduction was necessary as the total strain-based crack model overestimated the G modulus and therefore requires a reduction of the E-modulus in order to reach the same frequency as the linear orthotropic material model. For the modal analysis, this particular material model therefore behaves as the linear isotropic material model.
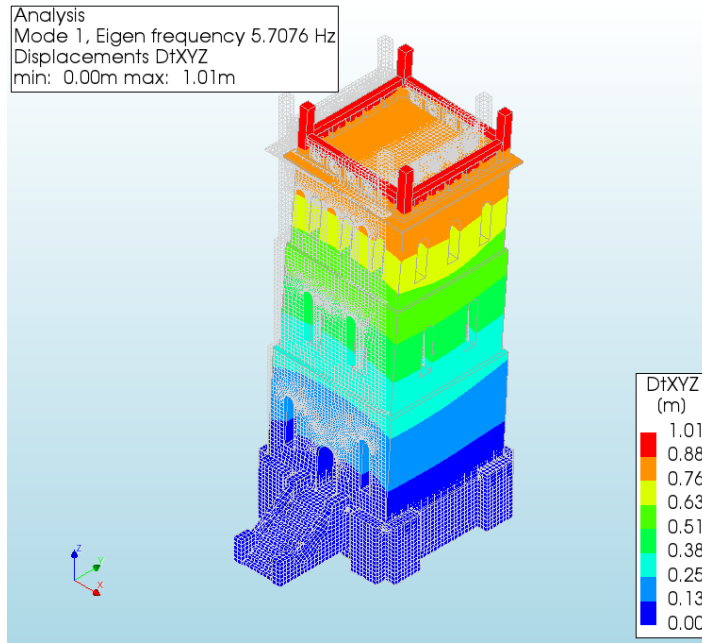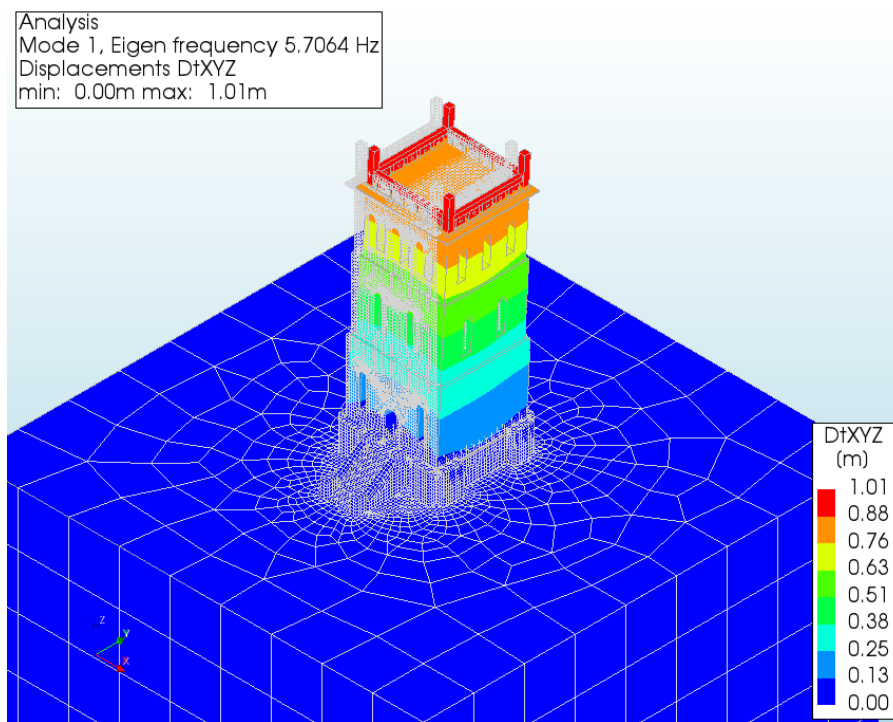
Figure 62 Mode 1 – nonlinear model without SSI

Figure 63 Mode 1 – nonlinear model with SSI

The results of the modal analysis for the model without SSI and with SSI for the nonlinear material models is presents in figure 62 and 63. The models are as seen, calibrated towards the first frequency of the tower.

_____

7.4.1 Pushover Analysis

To estimate the seismic structural deformations of a given structure, a nonlinear pushover method can be run. This can be done with the integrated pushover analysis module in Diana, by defining a modal load for a specific mode.

Table 12 Seismic impact analysis methods

Analysis of seismic impact			
Linear analysis		Nonlinear analysis	
Static	*Dynamic*	*Static*	*Dynamic*
Lateral force method	Response spectrum	**Pushover analysis**	Time history analysis

There are many different methods available for analysis in order to estimate the seismic impact, as presented in table 14. These methods range from linear and static to nonlinear and dynamic, where the static nonlinear pushover analysis is one the more popular methods to implement.

The pushover analysis allows for the evaluation of the structure's resistance to seismic impact where the analysis technique is based upon applying an increasing load monotonically until an aimed criterion for the analysis is set. This criteria is set through an aimed total displacement of the structure and thus predicting the load required for collapse of it [75].

The result of the performing a pushover analysis is the pushover curve as presented in figure 64, which indicates the maximum displacement on the structure for the given base shear (load). The curve can be used to show the capacity of the structure and the overall seismic strength.
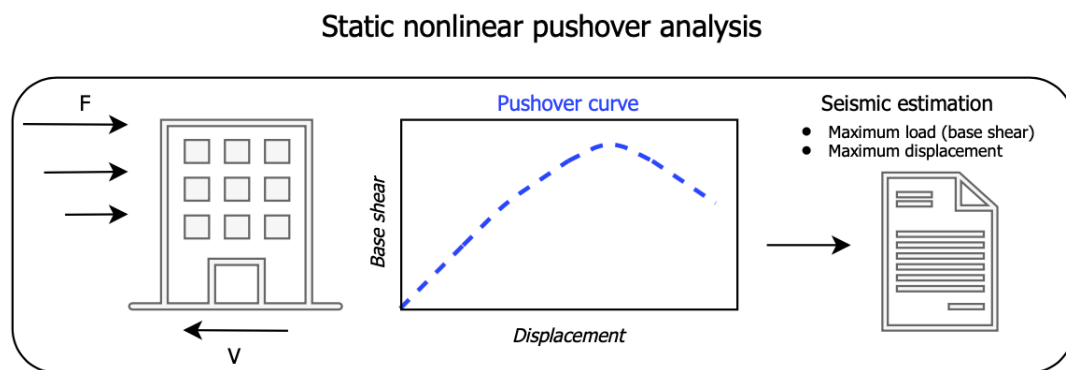

Figure 64 Pushover analysis procedure

While the analysis is not specifically difficult to implement on more simplified structures, the computational requirements of the analysis goes up drastically with different elements such as: complexity of a structure, mesh size, load step criteria on the analysis, and allowed tolerances.

Because of the needed computational requirements and lack of time, the nonlinear pushover analysis was not performed in this study. The reason is also related to the calibration, and the fact that only the first mode was assessed and therefore the calibration process did not in fact give a 100 % accurate representation of the structure.

Chapter 8: Conclusion and Future Work

8.1 Conclusion

The aim of this thesis was to identify the dynamic characteristics of the historical masonry tower located in the city of Tønsberg, Norway. In addition to modeling the same tower in a FE software. The identification was done with the use of the OMA and AVT, while the modeling of the tower was done with the use of 3D laser scanners.

The total extent of the thesis has provided an in depth look at different paths for OMA and AVT, including FE modeling and 3D laser scanning. While the situation (pandemic) during the thesis was not desirable for the work done, the results presented are of very interesting character.

The calibration process of the tower showed that the initial geometrical modeling of the structure was good, and the use of the 3D laser scanners were a great contribution to achieving this. Material properties of the stone masonry did indeed have a huge impact in the results of the analyzes. The results for the final modal analysis on the models showed a difference in the E-modulus at around 45 %, while other factors such as the soil and interface also had an impact on the results. The implementation of SSI can give a bigger factor of safety than expected which was also the case in this study, where the model with SSI gave consequentially lower natural frequencies. Therefore, when considering the two models, the model without SSI is more conservative.

The results of the modal analysis were also affected by the chosen material models. The linear material models showed different results for the isotropic and orthotropic model, while this difference was also present for the nonlinear material models. The reason for this was the estimation of the G-modulus, for both the nonlinear model and isotropic material model.

Both the models where calibrated to the first natural frequency of the tower, as extracted from the AVT. It is however not possible to take any concluding remarks on the robustness and accuracy of either of the models, as the FE models were only calibrated towards the first frequency. Challenges in the modelling of the structure and the conversion of point clouds into a usable FE model showed to be a difficult task. The lack of automation in the process caused unexpected difficulties in the meshing and some geometry had to be removed to allow for this to be done. The proceeding analysis of the non-linear models to find the pushover curves was also not preformed due to lack of time, however based on the ambient vibration data the models should indeed act as the real structure when performing a pushover analysis, with respect to the first mode shape.

_____

8.2 Future Works

- The most interesting conduit for the future is to assess the Slottsfjell tower once again, but more thoroughly. The study should look more in depth on the different materials used in the tower, with the execution of nondestructive tests on them. This testing should be conducted to verify the material and therefore make a more accurate model. More time should be used to model the structure and thus giving a more precise result. The modeling should put more emphasis on the foundation and the interaction of it with the tower itself. Because there are many insecurities in modeling of historical structure, more time will allow for more extensive calibration of the model, and consequently give a more precise result. Another part of the study should also investigate the OMA and how to perform and extract the data of the AVT in an easy and effective way.

- This thesis has also given the basis of using laser scanners as a use case for modeling historical structures, for the procedure in modal analysis. This is therefore an interesting work path that can be assed in the further, both for finding more automatic systems from the 3D laser scanning to final 3D shapes, but also specifically achieving higher precision in the non-automatic systems.

- Another element of interest that should be looked more into in the future is modelling of masonry structures. More specifically, historical stone masonry as the one presented in this thesis. While there are several studies into this, it is still lacking when compared to more established masonry types like regular brick masonry.

References

1.   Ulriksen, E., *Tønsberg-bebyggelse og beboere fra 1000-tallet til 1200-tallet.* UBAS Nordisk 5. De første 200 årene-nytt blikk på 27 skandinaviske middelalderbyer, 2008.

2.   DianaFEA, *Diana Solutions for Masonry & Historical Structures.* 2020.

3.   Shimpi, V., M.V. Sivasubramanian, and S. Singh, *System Identification of Heritage Structures Through AVT and OMA: A Review.* BIOCELL, 2019. **13**(1).

4.   Ren, W.-X. and Z.-H. Zong, *Output-only modal parameter identification of civil engineering structures.* Structural Engineering and Mechanics, 2004. **17**(3-4): p. 429-444.

5.   Foti, D., S. Ivorra, and M.F. Sabbà, *Dynamic investigation of an ancient masonry bell tower with operational modal analysis: A non-destructive experimental technique to obtain the dynamic characteristics of a structure.* 2012.

6.   Fu, Z.-F. and J. He, *Modal analysis.* 2001: Elsevier.

7.   Brincker, R. and C. Ventura, *Introduction to Operational Modal Analysis.* 2015: Wiley.

8.   Hetland, R., *Operational modal analysis of the Dolmsundet Bridge during construction.* 2015, NTNU.

9.   Schanke, S.A., *Operational modal analysis of large bridges.* 2015, NTNU.

10.   Kvåle, K.A., O. Øiseth, and A. Rønnquist, *Operational modal analysis of an end-supported pontoon bridge.* Engineering Structures, 2017. **148**: p. 410-423.

11.   Knutzen, A.N. and J.-A.B. Sivertsen, *Dynamic Identification and Modelling of a Pantograph.* 2018, NTNU.

12.   Foti, D., et al. *Output-only structural identification of the Engineering Faculty Edifice A at L'Aquila.* in *Conference Proceeding of the 4th International Operational Modal Analysis Conference IOMAC 2011.* 2011.

13.   Brincker, R., *Some elements of operational modal analysis.* Shock and Vibration, 2014. **2014**.

14.   Rainieri, C. and G. Fabbrocino, *Operational modal analysis of civil engineering structures.* Springer, New York, 2014. **142**: p. 143.

15.   Ghalishooyan, M. and A. Shooshtari. *Operational modal analysis techniques and their theoretical and practical aspects: A comprehensive review and introduction.* in *6th International Operatiional Modal Analysis Conference IOMAC 2015.* 2015.

16. Bayraktar, A., et al., *Ambient vibration tests of a steel footbridge.* Journal of Nondestructive Evaluation, 2010. **29**(1): p. 14-24.
17. Wikimedia, *Second order transfer function.* 2020.
18. Steven W. Smith, P.D. *Chapter 8: The Discrete Fourier Transform.* [cited 2020 13.05.2020]; Available from: https://www.dspguide.com/ch8/1.htm.
19. Lamb, M. and V. Rouillard. *Some issues when using Fourier analysis for the extraction of modal parameters.* in *Journal of Physics: Conference Series.* 2009. IOP Publishing.
20. Cochran, W.T., et al., *What is the fast Fourier transform?* Proceedings of the IEEE, 1967. **55**(10): p. 1664-1674.
21. Cooley, J.W. and J.W. Tukey, *An algorithm for the machine calculation of complex Fourier series.* Mathematics of computation, 1965. **19**(90): p. 297-301.
22. Slottsfjellsmuseet, *Slottsfjellstårnet.* 2020.
23. Peeters, B. and G. De Roeck, *Reference-based stochastic subspace identification for output-only modal analysis.* Mechanical systems and signal processing, 1999. **13**(6): p. 855-878.
24. Van Overschee, P. and B. De Moor, *Continuous-time frequency domain subspace system identification.* Signal Processing, 1996. **52**(2): p. 179-194.
25. Gentile, C., A. Saisi, and A. Cabboi, *Structural identification of a masonry tower based on operational modal analysis.* International Journal of Architectural Heritage, 2015. **9**(2): p. 98-110.
26. Venanzi, I., et al., *Contionous OMA for Damage Detection and Lo-Calization in the Sciri Tower in Perugia, Italy.* 2019.
27. Cavalagli, N., et al., *Detecting earthquake-induced damage in historic masonry towers using continuously monitored dynamic response-only data.* Procedia engineering, 2017. **199**: p. 3416-3421.
28. Ramos, L.F., et al., *Monitoring historical masonry structures with operational modal analysis: two case studies.* Mechanical systems and signal processing, 2010. **24**(5): p. 1291-1305.
29. Bayraktar, A., et al., *Seismic response of a historical masonry minaret using a finite element model updated with operational modal testing.* Journal of vibration and control, 2011. **17**(1): p. 129-149.
30. Ghiassi, B. and G. Milani, *Numerical Modeling of Masonry and Historical Structures: From Theory to Application.* 2019: Woodhead Publishing.
31. Magenes, G., et al. *Experimental characterisation of stone masonry mechanical properties.* in *Proc. 8th International Masonry Conference.* 2010. Dresden.

32. Yön, B., E. Sayın, and O. Onat, *Earthquakes and structural damages.* Earthquakes-Tectonics, Hazard and Risk Mitigation, 2017: p. 319-339.

33. Liu, G.-R. and S.S. Quek, *The finite element method: a practical course.* 2013: Butterworth-Heinemann.

34. Asteris, P.G., et al., *Numerical modeling of historic masonry structures*, in *Handbook of research on seismic assessment and rehabilitation of historic structures.* 2015, IGI Global. p. 213-256.

35. Giordano, A., E. Mele, and A. De Luca, *Modelling of historical masonry structures: comparison of different approaches through a case study.* Engineering Structures, 2002. **24**(8): p. 1057-1069.

36. Lourenço, P.B., *Computations on historic masonry structures.* Progress in Structural Engineering and Materials, 2002. **4**(3): p. 301-319.

37. Lou, M., et al., *Structure–soil–structure interaction: Literature review.* Soil Dynamics and Earthquake Engineering, 2011. **31**(12): p. 1724-1731.

38. Silvestri, F. and N. Moraci, *Earthquake Geotechnical Engineering for Protection and Development of Environment and Constructions: Proceedings of the 7th International Conference on Earthquake Geotechnical Engineering,(ICEGE 2019), June 17-20, 2019, Rome, Italy.* 2019: CRC Press.

39. Shabani, A. and S. Erfani, *Seismic Performance Evaluation of SSMF with Simple Beam–Column Connections Under the Base Level.* International Journal of Steel Structures, 2020. **20**(1): p. 89-100.

40. Givens, M.J., et al., *Assessment of soil-structure interaction modeling strategies for response history analysis of buildings.* 2012.

41. Yang, H., X. Xu, and I. Neumann, *Laser scanning-based updating of a finite-element model for structural health monitoring.* IEEE Sensors Journal, 2015. **16**(7): p. 2100-2104.

42. Barazzetti, L., et al., *BIM from laser clouds and finite element analysis: combining structural analysis and geometric complexity.* 2015.

43. Autodesk. *Autodesk Revit.* [cited 2020 13.06.2020]; Available from: https://www.autodesk.com/products/revit/.

44. Graphisoft. *ArchiCAD.* [cited 2020 13.06]; Available from: https://www.graphisoft.com/archicad/.

45. Lubowiecka, I., et al., *Historic bridge modelling using laser scanning, ground penetrating radar and finite element methods in the context of structural dynamics.* Engineering Structures, 2009. **31**(11): p. 2667-2676.

46. Hinks, T., et al., *Point cloud data conversion into solid models via point-based voxelization.* Journal of Surveying Engineering, 2013. **139**(2): p. 72-83.

47. Armesto, J., et al., *Modelling masonry arches shape using terrestrial laser scanning data and nonparametric methods.* Engineering Structures, 2010. **32**(2): p. 607-615.

48. Bucher, F., *Medieval architectural design methods, 800-1560.* Gesta, 1972. **11**(2): p. 37-51.

49. Stylegar, F.-A., *Osebergfunnet.* 2019.

50. Shan, J. and C.K. Toth, *Topographic laser ranging and scanning: principles and processing.* 2018: CRC press.

51. Topcon, *GLS-2000 Series Multi-Functional 3D Laser Scanner.* 2019.

52. Autodesk. *Autodesk Recap.* Available from: https://www.autodesk.com/products/recap/overview.

53. Exchanger, C. *CAD Exchanger.* Available from: https://cadexchanger.com.

54. Shah, C. *Mesh discretization error and criteria for accuracy of finite element solutions.* in *Ansys users conference.* 2002.

55. Ma, G., H. Hao, and Y. Lu, *Homogenization of masonry using numerical simulations.* Journal of engineering mechanics, 2001. **127**(5): p. 421-431.

56. Rosenqvist, I.T., *Electron-microscope investigations of larvikite and tönsbergite feldspars.* Norsk geologisk tidsskrift, 1965. **45**(1): p. 69-71.

57. Petersen, J.S., *Structure of the larvikite-lardalite complex, Oslo-region, Norway, and its evolution.* Geologische Rundschau, 1978. **67**(1): p. 330-342.

58. DianaFEA, *Transient Dynamic Analysis of a Machine Foundation.*

59. Castro-Triguero, R., et al., *Robustness of optimal sensor placement under parametric uncertainty.* Mechanical Systems and Signal Processing, 2013. **41**(1-2): p. 268-287.

60. Kirkegaard, P.H., *Optimal design of experiments for parametric identification of civil engineering structures.* 1991, Dept. of Building Technology and Structural Engineering, Aalborg University.

61. Pastor, M., M. Binda, and T. Harčarik, *Modal assurance criterion.* Procedia Engineering, 2012. **48**: p. 543-548.

62. Guratzsch, R.F. and S. Mahadevan, *Structural health monitoring sensor placement optimization under uncertainty.* AIAA journal, 2010. **48**(7): p. 1281-1289.

63. Sun, H. and O. Büyüköztürk, *Optimal sensor placement in structural health monitoring using discrete optimization.* Smart Materials and Structures, 2015. **24**(12): p. 125034.

64. Cantieni, R. *Experimental methods used in system identification of civil engineering structures.* in *Proceedings of the International Operational Modal Analysis Conference (IOMAC).* 2005.

65.   Lopez, S., et al., *Simplified formulation for estimating the main frequencies of ancient masonry churches.* Front. Built Environ, 2019. **5**: p. 18.

66.   ASCE, *ASCE/SEI 7 Minimum Design Loads For Buildings and Other Structures.*

67.   Borri, A. and A. De Maria. *Eurocode 8 and Italian Code. A comparison about safety levels and classification of interventions on masonry existing buildings.* in *Eurocode 8 Perspectives from the Italian Standpoint Workshop.* 2009.

68.   Unquake. *Products.* [cited 2020 08.03]; Available from: https://www.unquake.co/products.

69.   MathWorks. *MATLAB.* Available from: https://www.mathworks.com/products/matlab.html.

70.   Milani, G. and F. Clementi, *Advanced Seismic Assessment of Four Masonry Bell Towers in Italy after Operation Modal Analysis (OMA) Identification.* International Journal of Architectural Heritage, 2019: p. 1-30.

71.   Felix, L., *Compressive strength and modulus of elasticity of masonry prisms.* Master of engineering Thesis, Departement of Civil and Environmental Engineering, Carleton University, Canada, 1999.

72.   Zaid, M., et al. *Effect of staircase on RC frame structures under seismic load.* in *International Conference on Trends and Challenges in Concrete Structures, Ghaziabad, UP, India, December.* 2013.

73.   Singh, N.S. and S. Choudhury, *Effects of staircase on the seismic performance of RCC frame building.* International Journal of Engineering Science and Technology, 2012. **4**(4).

74.   DianaFEA, *Nonlinear Pushover Analysis of a Masonry Building with DIANA.*

75.   GARCIA, H.A., *Modal pushover analysis for seismic vulnerability analysis.* 2014.

Appendix

_____

A – Sensor Specifications

Type	20-bit Low Noise, Low Drift, Low Power, 3-Axis MEMS Digital Accelerometer
Range	±2.048 g, ±4.096 g, and ±8.192 g
X-Axis, Y-Axis, and Z-Axis Sensitivity (LSB/g)	±2 g: 235,520 256,000 276,480 ±4 g: 117,760 128,000 138,240 ±8 g: 58,880 64,000 69,120
Noise density	25 µg/√Hz
Sampling rates (ODR) and Low-Pass Filtering	500 Hz and 125 Hz 250 Hz and 62.5 Hz 125 Hz and 31.25 Hz 62.5 Hz and 15.625 Hz 31.25 Hz and 7.813 Hz 15.625 Hz and 3.906 Hz 7.813 Hz and 1.953 Hz 3.906 Hz and 0.977 Hz
High-Pass Filtering	No filter 247 × 10−3 × ODR 62.084 × 10−3 × ODR 15.545 × 10−3 × ODR 100 3.862 × 10−3 × ODR 0.954 × 10−3 × ODR 0.238 × 10−3 × ODR
Connectivity	Up to 1 meter cable for connection

Figure A. 1 Sensor specifications

B – AVT Results

Initial reading

x-direction	y-direction

Sensor 1
No data

Sensor 2
No Data

Sensor 3
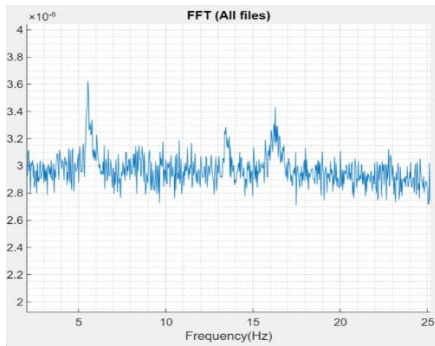
Figure B. 1 Sensor 3 x-direction - initial reading
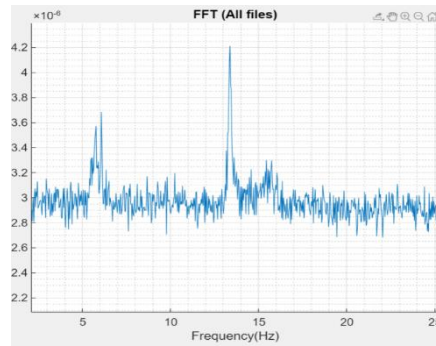
Figure B. 2 Sensor 3 y-direction - initial reading

Sensor 4
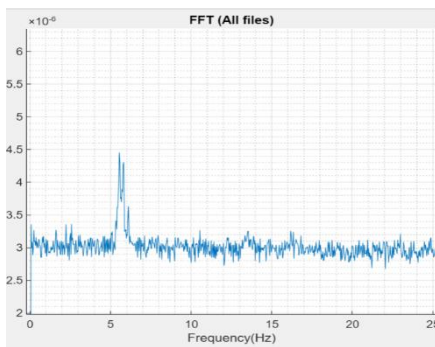
Figure B. 3 Sensor 4 x-direction - initial reading
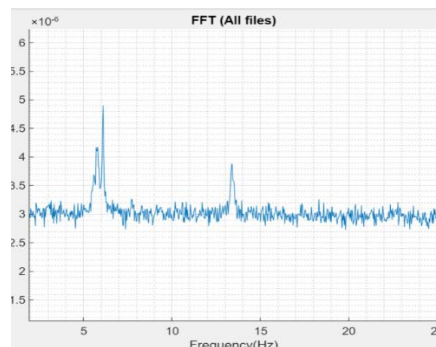
Figure B. 4 Sensor 4 y-direction - initial reading

_____

| x-direction | y-direction |

Sensor 5
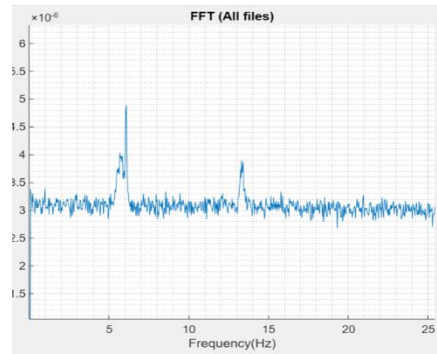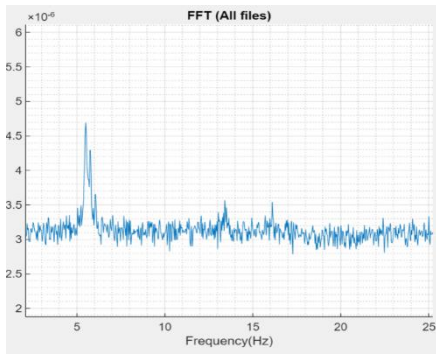
Figure B. 5 Sensor 5 x-direction - initial reading

Figure B. 6 Sensor 5 y-direction - initial reading
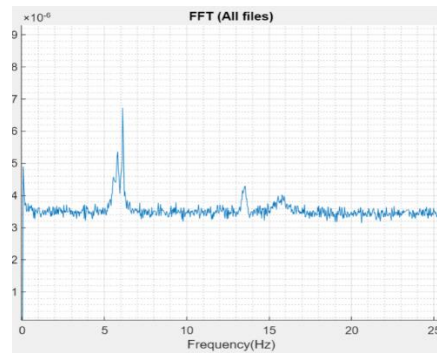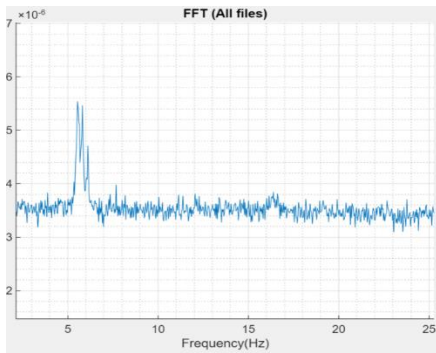
Sensor 6

Figure B. 7 Sensor 6 x direction - initial reading

Figure B. 8 Sensor 6 y-direction - initial reading

Sensor 7
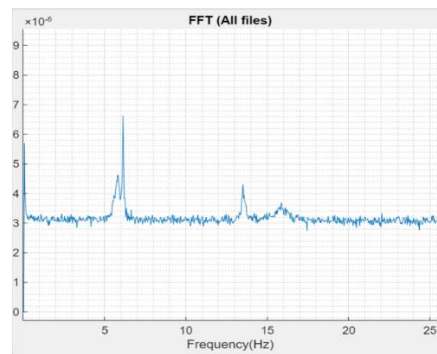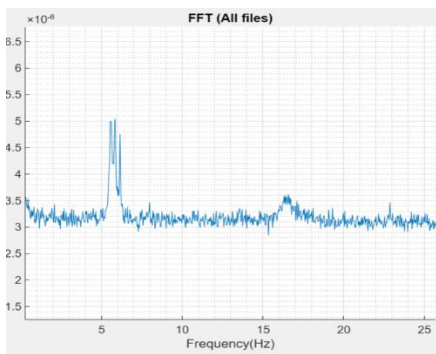
Figure B. 9 Sensor 7 x-direction - initial reading

Figure B. 10 Sensor 7 y-direction - initial reading

Second reading

x-direction	y-direction
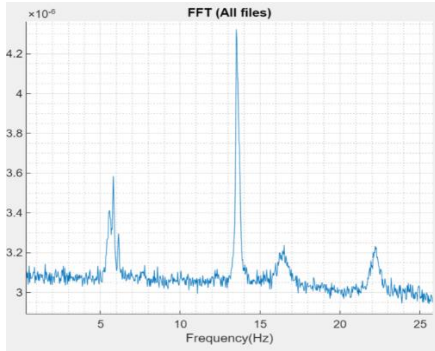
Sensor 1

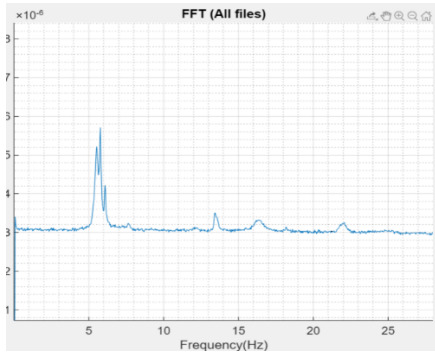*Figure B. 11 Sensor 1 x-direction - second reading*
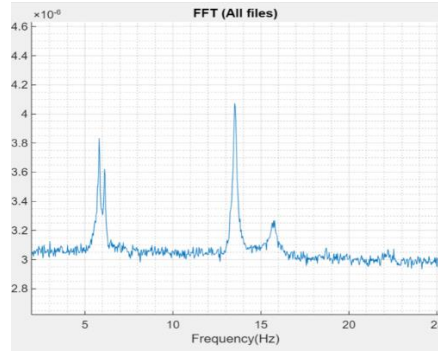
Figure B. 12 Sensor 1 y-direction - second reading

Sensor 2
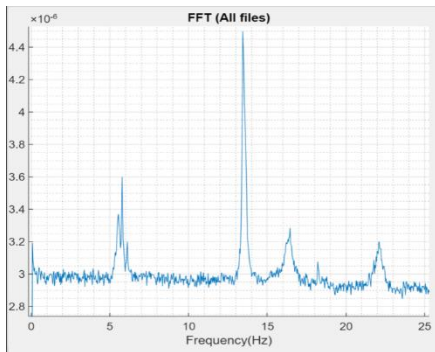
Figure B. 13 Sensor 2 x-direction - second reading
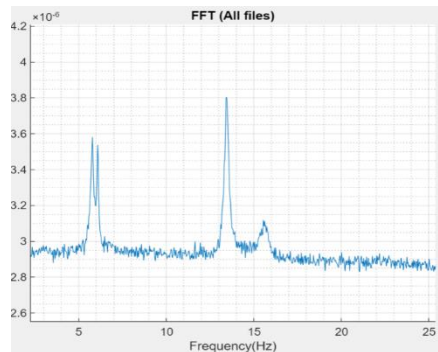
Figure B. 14 Sensor 2 y-direction - second reading
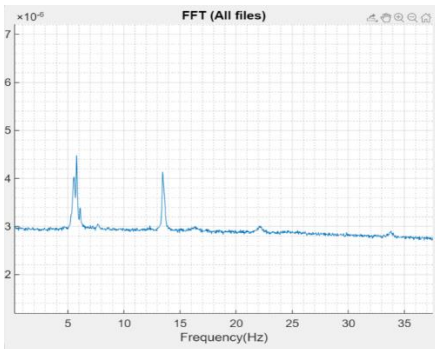
Sensor 3
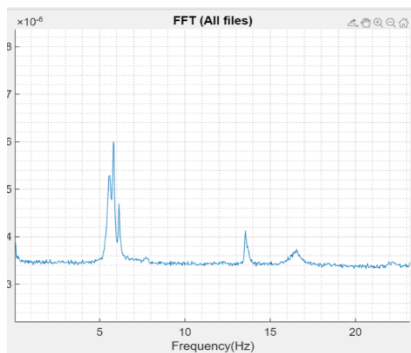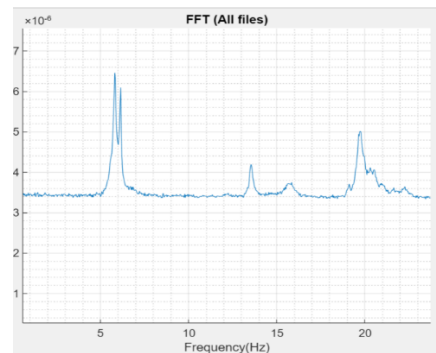

Figure B. 15 Sensor 3 x-direction - second reading
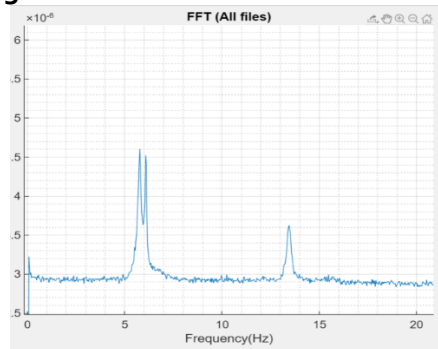
Figure B. 16 Sensor 3 y-direction - second reading

_____

| x-direction | y-direction |

Sensor 4
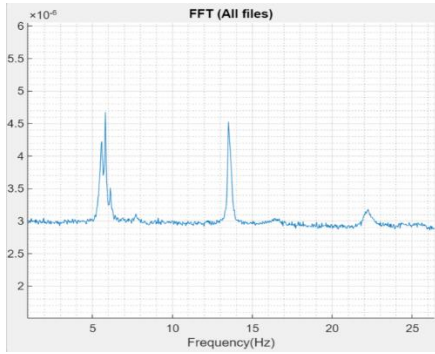
Figure B. 17 Sensor 4 x-direction - second reading
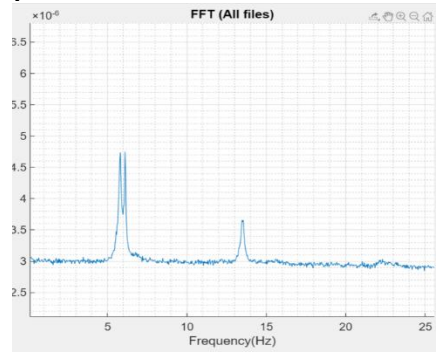
Figure B. 18 Sensor 4 y-direction - second reading

Sensor 5

Figure B. 19 Sensor 5 x-direction - second reading

No data

Sensor 6

Figure B. 20 Sensor 6 x-direction - second reading

Figure B. 21 Sensor 6 y-direction - second reading
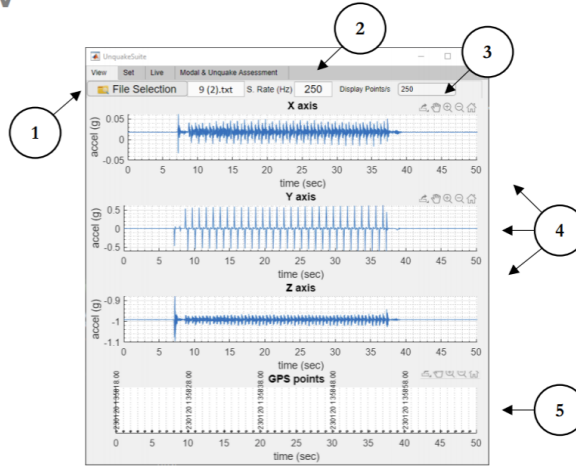
C – Software Overview

3.3 View

Figure 6 View tab

|		
1 File Selection		Select the .txt file you want to open. It should follow the Unquake Accelerograph format.
2 S.Rate (Hz)		The sampling rate of measurements in the opened .txt file. It is written in the first line of each file from Unquake Accelerograph.
3 Display Points/s		A performance wise dropdown menu to select the <u>displaying</u> equivalent of S.Rate value. If you want to see every measurement on the screen, it should match the S.Rate(Hz). Smaller values provide faster visualization of the signal. Note: When no file is open, change the value to open a new file. Otherwise, it reloads the file according to the shown Display Points/s
4 Acceleration time-histories		The acceleration time-histories of the three sensor's local axes (as shown in sensor housing).

Figure C. 1 Software interface 01

SOFTWARE OVERVIEW

3.4 Set

Figure 7 Set tab

A
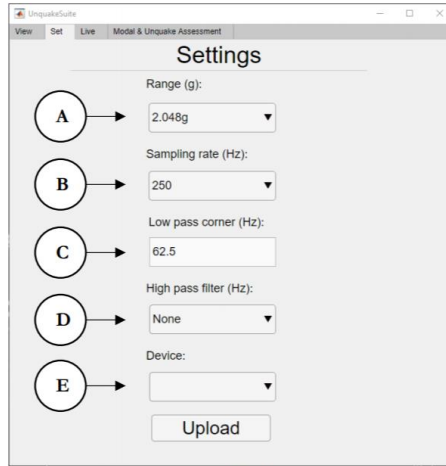
Range (g)

Dropdown menu to select from the available ranges:
- +/- 2.048g
- +/- 4.096g
- +/- 8.192g

B

Sampling rate (Hz)

Dropdown menu to select from the available sampling rates. Sampling rate is practically how many points per second you capture with the sensor from the continuous-time signal. **Recommended value**: 250Hz.

Note: For **500Hz** sampling rate there is **no GPS support**.

C

Low pass corner (Hz)

Showing the value of the low pass corner of the digital filter. It can't be altered and it derives from the Sampling Rate value divided by four.

D

High pass filter (Hz)

Dropdown menu to select from the available High pass filter (Hz) options.

Figure C. 2 Software interface 02

SOFTWARE OVERVIEW

E
Device

Dropdown menu to select which of the available COM devices will be configured. Each Unquake Accelerograph is recognized as a COM device in your Windows machine.

Note: If you plugged the device while being in Set tab, then change tab in order to refresh the list.

Note

⚠ **Separate files of 20min duration** are created in microSD card independently of the configuration. Keep in mind each time device is powered on (even through USB), it creates a new file.

3.5 Live

Figure 8 Live tab

1
Device
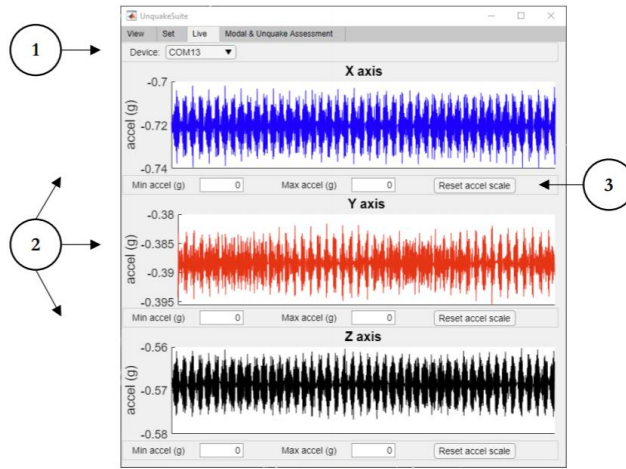
Select the device you want to see live time-histories.

Figure C. 3 Software interface 03

SOFTWARE OVERVIEW

2

Live acceleration time-histories

The acceleration time-histories of the three sensor's local axes (as shown in sensor housing) in real-time.

3

Graph scale panel

Control graph scale by setting a minimum/maximum acceleration value for plot area. If you want to return to auto scale mode, click "Reset accel scale".
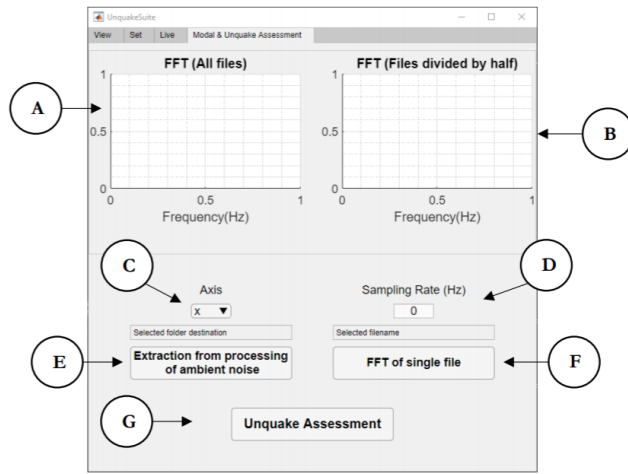
3.6 Modal & Unquake Assessment

Figure 9 Modal & Unquake Assessment tab

A

FFT (All files) Graph

Graph area where Fast Fourier Transform Amplitudes are shown either from all files of the folder selected through "Extraction from processing of ambient noise" or from the single file through "FFT of single file".

B

FFT (Files divided by half) Graph

Graph area where **two** - Fast Fourier Transform Amplitudes lines are shown for the files contained in the folder selected through "Extraction from processing of ambient noise". Those files are divided by half in two same total-time duration bins.

Note: Useful to check if a frequency stays the same between those two time periods.
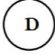
19

Figure C. 4 Software interface 04

S O F T W A R E   O V E R V I E W

(C)

Graph scale panel

Dropdown menu to select the local sensor's axis of interest before proceeding to *D* or *E*.

(D)

Sampling Rate (Hz)

The sampling rate of measurements in the opened .txt file. It is written in the first line of each file from Unquake Accelerograph.

(E)

Extraction from processing of ambient noise (Optional)

Stacking and performing Fourier transform on hundreds of files imported from accelerograph providing Fourier transform amplitudes. This applies to ambient noise measurements, which are distinguished from all those not subject to the assumption of white noise, such as stronger local (and not) excitations. - **Internet connection is required.**

Note: **Ensure** all the **.txt** files inside the selected folder have the Unquake Accelerograph's format. Other files or folder inside do not conflict the procedure.

(F)

FFT of single file

Fast Fourier Transform of a single file.

(G)

Unquake Assessment (Optional)

Pre-seismic assessment of buildings by combining the accelerograph measurements with typical building push over curves extracted from verified databases (like that provided in FEMA's HAZUS) as the user inputs the basic building characteristics like material and type, year of design and construction, seismic regulation, height, location and/or soil – foundation characteristics. - **Internet connection is required.**

Note

⚠ For "Extraction from processing of ambient noise" or/and "Unquake Assessment" you will be for a separate license. These licenses are called as **license_ambient.dat** and **license_unquake.dat** respectively. The first time you click one of these features, a prompt window will be shown asking you to select the corresponding license file.

20

Figure C. 5 Software interface 05

D - AVT and Laser Scanning

Figure D. 1 Sensor 1 – second reading

Figure D. 2 Sensor 2 – second reading

_____

Figure D. 3 Sensor 3 – second reading

Figure D. 4 Sensor 4 – second reading
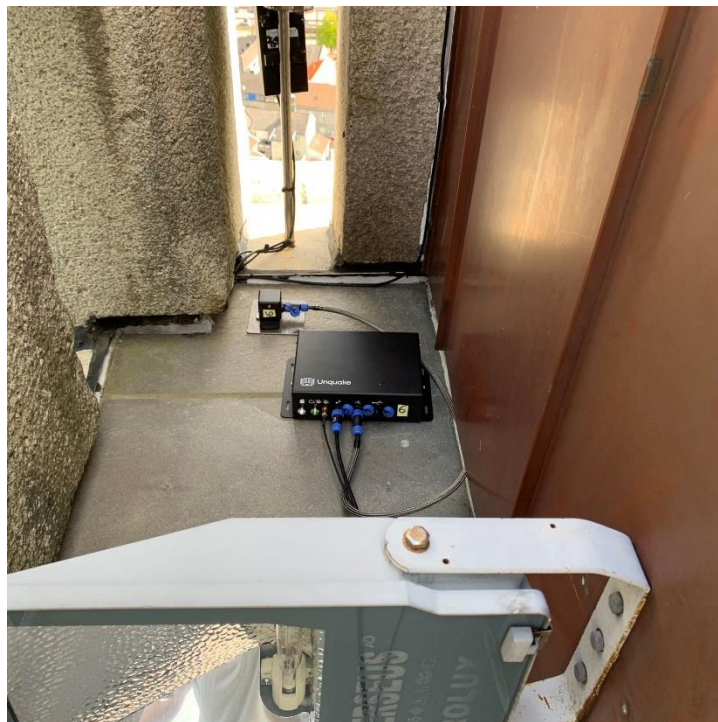
Figure D. 5 Sensor 5 – second reading

Figure D. 6 Sensor 6 – second reading

_____

Figure D. 7 3D laser scanning 01

Figure D. 8 3D laser scanning 02